

AGEDI | THE ABU DHABI GLOBAL ENVIRONMENTAL DATA INITIATIVE

CLIMATE CHANGE PROGRAMME

REGIONAL CLIMATE CHANGE: ATMOSPHERIC MODELLING

Atmospheric  
Modelling

Arabian Gulf  
Modelling

Terrestrial  
Ecosystems

Marine  
Ecosystems

Transboundary  
Groundwater

Water Resource  
Management

Al Ain Water  
Resources

Coastal  
Vulnerability Index

Desalinated  
Water Supply

Food Security

Public Health Benefits  
of GHG Mitigation

Sea Level Rise



مبادرة أبوظبي العالمية للبيانات البيئية  
Abu Dhabi Global Environmental Data Initiative

Suggested Citation: AGEDI. 2015. Regional Atmospheric Modeling- Future Scenarios. LNRCCP. NCAR/CCRG

This report was prepared as an account of work sponsored by the Abu Dhabi Global Environmental Data Initiative (AGEDI). AGEDI neither makes any warranty, express or implied, or assumes any legal liability or responsibility for the accuracy, completeness, nor usefulness of the information provided. The views and opinions of authors expressed herein do not necessarily state or reflect those of the EAD or AGEDI.



## Acknowledgments

Many individuals provided invaluable support, guidance, and input to the Modeling projects.

The authors would like to express their sincere and heartfelt expressions of gratitude for their review by providing comments, feedback, data and/or the opportunity to present multiple deliverables within the project process including:

Dr. Abdulla Al Mandoos, National Centre of Meteorology and Seismology

Dr. Fred Launay and the Environment Agency- Abu Dhabi team

Dr. Holger Hoff, Stockholm Environment Institute

Dr. Mansour Al Mazroui, Centre of Excellence for Climate Change Research (CECCR)

Mr. Mufleh Alalaween, IUCN ROWA

Ms. Naoko Kubo, UAE Ministry of Environment and Climate Change (MOCCA) and team

Dr. Omar Abdullah, National Centre of Meteorology and Seismology

Dr. Paola Ferreira and the Emirates Wildlife Society (EWS) – WWF team

Dr. Rachel McDonnell, International Centre for Biosaline Agriculture (ICBA)

Dr. Robert Baldwin and Dr. Simon Wilson, Five Oceans

Dr. Saeed Al Sarmi, Research Centre from Public Authority for Civil Aviation (PACA)

Dr. Sultan Al Yahyai, Sultan Qaboos University

Dr. Tarek Sadek, UNESCWA

A very special thank-you to the academic scientific research teams of Khalifa University (KU), MASDAR Institute of Science and Technology (MIST), New York University (NYU) for your data expertise and scientific feedback, support and opportunities for further research.

We are additionally thankful the participation, time and effort that multiple stakeholders across the region who participated in the multitude of meetings and dialogue.

## About this Final Report

In October 2013, the Environment Agency of Abu Dhabi launched the "Local, National, and Regional Climate Change (LNRCC) Programme to build upon, expand, and deepen understanding of vulnerability to the impacts of climate change as well as to identify practical adaptive responses at local (Abu Dhabi), national (UAE), and regional (Arabian Peninsula) levels. The design of the Programme was stakeholder-driven, incorporating the perspectives of over 100 local, national, and regional stakeholders in shaping 12 research sub-projects across 5 strategic themes. The "Regional Atmospheric Modeling" sub-project within this Programme aims to develop high resolution, regional climate data that will serve the Climate Change Impacts, Vulnerability and Adaptation Assessment Activities for the Abu Dhabi Environment Agency, as well as organizations across the broader Arabian Peninsula

This is the final report which offers offer a summary of what has been learned in carrying out the research activities involved in the "Regional Atmospheric Modeling" sub-project. This report describes the methodological approach, data used to support the approach, and descriptions of specific and general findings. This report seeks to provide a useful synthesis of the work, and offers partners and stakeholders the opportunity to understand what was done, and request additional information. We also provide examples of add-on/derived data sets that could be extracted from the baseline data that we have developed for other Vulnerability and Adaptation Assessments.

The data archive we have generated is large. We estimate we have an archive of nearly 110 Terra-Bytes. Because of this large size, we believe it makes more sense to demonstrate the datasets that can be developed, and then work with our stakeholders to derive specific datasets that they might need for their studies. In this way, we hope other researchers can identify specific derived products that they might find useful, and that such a process would provide an opportunity to influence and/or directly affect subsequent research activities.



## Table of Contents

|  | <u>page</u> |
|--|-------------|
| <b>ABOUT THIS FINAL REPORT</b>   | <b>I</b>    |
| <b>LIST OF FIGURES</b>   | <b>IV</b>   |
| <b>LIST OF ACRONYMS</b>  | <b>VII</b>  |
| <b>1. SUMMARY OF FINDINGS</b>  | <b>8</b>    |
| <b>2. BACKGROUND</b>   | <b>12</b>   |
| 2.1. THE CLIMATE OF THE REGION   | 12          |
| 2.2. MOTIVATION, CONTEXT, GOALS AND OBJECTIVES                                       | 13          |
| 2.3. RESEARCH TEAM   | 16          |
| <b>3. OVERVIEW OF EXPERIMENT AND METHODOLOGICAL APPROACH</b>                         | <b>17</b>   |
| 3.1. THE GLOBAL CLIMATE MODEL CONTEXT  | 18          |
| <b>4. WRF SIMULATIONS OF CURRENT AND FUTURE CLIMATE</b>                              | <b>20</b>   |
| 4.1. WRF CLIMATE SIMULATIONS WITH ERA-INTERIM  | 21          |
| 4.2. WRF CLIMATE SIMULATIONS WITH CCSM4 (BOUNDARY FORCING)                           | 25          |
| 4.3. SIMULATED REGIONAL CLIMATE FOR THE CONTEMPORARY PERIOD                          | 26          |
| 4.4. PROJECTIONS OF FUTURE CLIMATIC CHANGE WITH CCSM4                                | 34          |
| 3.1 CHANGES IN WIND AROUND ABU DHABI ISLAND  | 44          |
| 4.5. A CLIMATE ANOMALY IN THE CCCSM4 FORCING AND ITS IMPLICATION FOR THE WRF RESULTS | 46          |
| <b>5. SUMMARY</b>  | <b>49</b>   |
| <b>6. REFERENCES</b>   | <b>51</b>   |
| <b>ANNEX: DESCRIPTION OF SOFTWARE FOR GENERATING WRF INTERMEDIATES</b>               | <b>53</b>   |

## List of Figures

|  | <u>page</u> |
|--|-------------|
| Figure 3. Overview of Concept Proposals and the representation of their inter-connectedness. ....  | 14          |
| Figure 5. Domains used in WRF simulations. ....  | 19          |
| Figure 6. <i>The Experimental Design. WRF was run for 20 and 10 years for the contemporary period and the future period at 12 and 36 km; and 4-km, respectively.</i> ....  | 21          |
| Figure 7. WRF rainfall biases (color-coded dots), WRF rainfall (mm, color shading), and WRF terrain height (gray contours) for July 1995 for subset of domain in Fig. 1. ....  | 22          |
| Figure 8. Same as (a) except for December 1995. ....   | 22          |
| Figure 9. Daily rainfall tendencies for selected locations for December 1995. Observed tendencies in blue and WRF tendencies in red. ....  | 23          |
| Figure 10. A sample case of diurnal cycle of 2-m air temperature from D03, which is the 4-km domain. Upper left 00:00 Local, 02:00 local upper middle, 04:00 upper right; and 22:00 low right. ....  | 24          |
| Figure 11. Mean precipitation anomaly from the full suite of GCMs from the IPCC AR5 experiment for the Arabian Peninsula region. ....  | 26          |
| Figure 12. Projected change in the precipitation anomaly for the CCSM model, which includes multiple ensemble members. Some ensemble members included very long runs past 2100, which extend to 2300. ....   | 27          |
| Figure 13. Annual precipitation estimates from a) the UAE Rainfall Atlas, b) NASA's TRMM sensor (~25 km resolution; 1999-2011 average), c) the CPC CMORPH product (~8 km resolution; 2003-2009 average), d) the WRF "Baseline" simulations driven by ERA-Interim (12-km resolution, 1986-2005 average), and e) the WRF 20THC simulations driven by CESM (12-km resolution, 1986-2005 average). ....  | 29          |
| Figure 14. Average monthly observed (various periods) versus modeled (1986-2005) temperature in five UAE cities. Observed temperature records are obtained from the Dubai Meteorological Office (Dubai), the National Oceanic and Atmospheric Administration (Abu Dhabi, Sharja and Ras al-Kaimah), and www.myweather2.com (Fujairah). Error bars and shading indicate standard deviations of monthly means, with the observed standard deviation values are assumed to be the same as for the WRF 12-km baseline, because data were not available. .... | 31          |
| Figure 15. Same as Figure 14, but for precipitation. ....  | 32          |
| Figure 16. Annual precipitation estimates for the entire 12-km domain and from a) NASA's TRMM sensor (~25 km resolution; 1999-2011 average), b) the CPC CMORPH product (~8 km resolution; 2003-2009 average), c) the WRF "Baseline" simulations driven by ERA-   |             |

|   |    |
|---|----|
| Interim (12-km resolution, 1986-2005 average), and d) the WRF 20THC simulations driven by CESM (12-km resolution, 1986-2005 average).....   | 33 |
| Figure 17. Annual precipitation estimates for the entire 36-km domain and from a) NASA's TRMM sensor (~25 km resolution; 1999-2011 average), b) the CPC CMORPH product (~8 km resolution; 2003-2009 average), c) the WRF "Baseline" simulations driven by ERA-Interim (12-km resolution, 1986-2005 average), and d) the WRF 20THC simulations driven by CESM (12-km resolution, 1986-2005 average)..... | 34 |
| Figure 18. WRF precipitation estimates for the 20THC simulation (left column), RCP 8.5 simulation (center column), and the difference (percentage change of RCP 8.5 minus 20THC; right column). Top row is averaged for winter (December, January, and February) bottom row is averaged for summer (June, July and August).....   | 35 |
| Figure 19. Annual average monthly precipitation for 20THC (1986-2005) versus future RCP4.5 (2060-2079) simulations in five UAE cities. Future changes in precipitation that are statistically significant are indicated by dots near the top of each graph, the color of which indicates the level of significance (see legend). Error bars indicate standard deviations of monthly means. ....         | 37 |
| Figure 20. Same as Figure 19, but for the RCP8.5 scenario. ....   | 38 |
| Figure 21. Wet Days Index values (the number of days with rainfall greater than 1 mm, summed over the 20-year time periods), for 20THC (left), RCP 8.5 (center), and the difference (RCP 8.5 minus 20THC; right). ....  | 39 |
| Figure 22. Projected change in precipitation over the 36-km domain for the RCP4.5 and RCP8.5 .....  | 40 |
| Figure 23. Average DJF (top) and JJA (bottom) 2-m Air Temperature (°C), for 20THC (left), RCP 8.5 (center), and the difference (RCP 8.5 minus 20THC; right). ....   | 40 |
| Figure 24. Average DJF (top) and JJA (bottom) 2-m Specific Humidity (g/kg), for 20THC (left), RCP 8.5 (center), and the difference (RCP 8.5 minus 20THC; right).....  | 41 |
| Figure 25. Monthly average temperature for 20THC (1986-2005) versus future RCP4.5 (2060-2079) simulations in five UAE cities. Future changes in temperature that are statistically significant are indicated by dots near the top of each graph, the color of which indicates the level of significance (see legend). Error bars and shading indicate standard deviations of monthly means. ....        | 42 |
| Figure 26. Same as Figure 25, but for the RCP8.5 scenario. ....   | 43 |
| Figure 27. Heat Wave Duration Index values (the number of days, in intervals of 6 days, that the daily maximum temperature is greater than 5°C above a reference value), for 20THC (left), RCP 8.5 (center), and the difference (RCP 8.5 minus 20THC; right). ....  | 44 |
| Figure 28. Mean 10-m winds around Abu Dhabi Island for DJF, early morning local time (0600) (top) and the early evening local time (1800) (bottom).....   | 45 |

Figure 29. Mean 10-m winds around Abu Dhabi Island for JJA, early morning local time (0600) (top) and the early evening local time (1800) (bottom).....46

Figure 30. A future cyclone in the CCSM4 model that tracks first across the Arabian Sea and then the Arabian Peninsula, showing sea-level pressure for the color-composite grid and a minimum contour range of 950 to 995 (hPa) in black. The top-left image is for 13 September, the top-right image is for 14 September, etc. The bottom-right panel is for 18 September, when the event is over the Arabian Peninsula. ....47

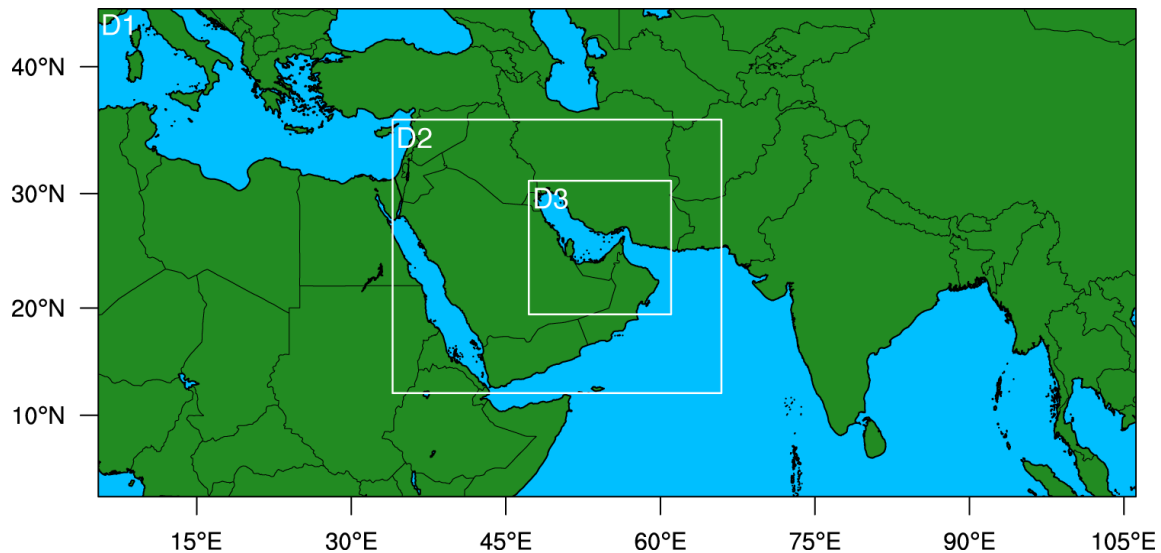
## List of Acronyms

|       |  |
|-------|--|
| AOGCM | Coupled Atmosphere Ocean General Circulation Model |
| AR5   | The 5 <sup>th</sup> Assessment Report of the IPCC  |
| CCSM4 | The NCAR Community Earth System Model Version 4    |
| CMIP5 | Climate Model Intercomparison Version 5            |
| EAD   | Environment Agency of Abu Dhabi                    |
| ECMWF | European Center for Medium Range Forecast          |
| FAR   | Fourth Assessment Report (IPCC)                    |
| GCM   | Global Climate Model                               |
| GHG   | Greenhouse gas                                     |
| GIS   | Geographic Information System                      |
| GoAD  | Government of Abu Dhabi                            |
| HWDI  | Heat Wave Duration Index                           |
| IPCC  | Intergovernmental Panel on Climate Change          |
| LNRCC | Local, National, and Regional Climate Change       |
| NCAR  | National Center for Atmospheric Research           |
| NWSC  | The NCAR-Wyoming Supercomputer or “Yellowstone”    |
| PI    | Principal Investigator                             |
| RCM   | Regional Climate Model                             |
| RCP   | Representative Concentration Pathway               |
| RT    | Research Team                                      |
| SST   | Sea Surface Temperatures                           |
| TAR   | Third Assessment Report (IPCC)                     |
| TRMM  | Tropical Rainfall Measurement Mission              |
| UAE   | United Arab Emirates                               |
| WRF   | Weather Research and Forecasting model             |
| 20THC | 20 <sup>th</sup> Century Climate Simulations       |



## Summary of Findings

The climate change vulnerability and adaptation assessment of the Abu Dhabi Environment Agency includes individual investigations that are exploring potential vulnerabilities, impacts, and adaptation options of various resource sectors, ecological systems, and human health. At different levels of need and requirement, each of these studies is making use of both current and future climate scenarios from which to undertake their research. This project generated a dataset of dynamically downscaled climate data of both the current and future climate through the deployment of a NCAR's Weather Research Forecast (WRF) model. The WRF model was used to dynamically downscale data from NCAR's Community Earth System Model Version 4 (CCSM4), resulting in a set of spatially consistent weather data across the Arabian Peninsula at resolutions of 36-km (D1), 12-km (D2) and 4-km (D3) (Fig S1).



**Figure S1. Domains used in the WRF simulations.**

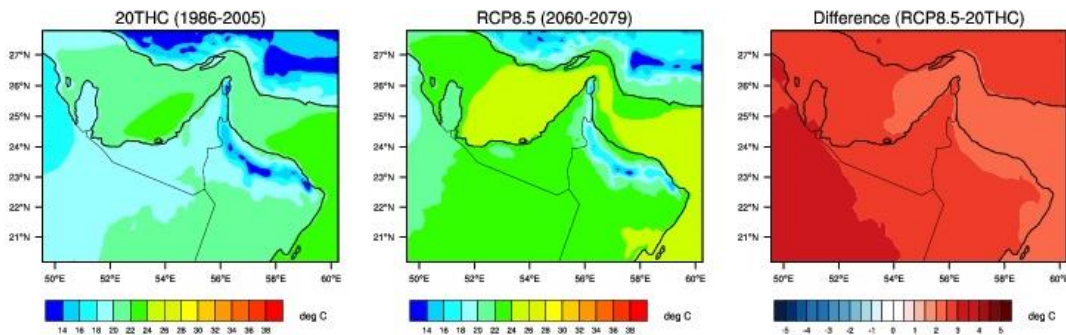
In a verification phase of this project, we report the skill of the WRF model in simulating the climate of the region, which was done by conducting 30-year baseline simulation for the historical period (20THC), forced by bias-corrected data from NCAR's Community Earth Systems Model (CCSM4). This WRF baseline captured the annual cycle of temperature reasonably well, with a cold bias of less than 1°C evident in the spring and early summer months, while there was a warm bias of about 3°C during the autumn and winter months. The cold-bias may be partly linked to a positive precipitation bias during the autumn winter months, which suggests that these baseline simulations may be cloudier than observed.

The WRF 20THC simulations that are driven by the bias-corrected CCSM4 dataset were shown to realistically resolve regional weather processes from a climatic perspective when compared to observations. The WRF model was shown to reasonably capture the magnitude of precipitation during January through October; however during November and December precipitation amounts are consistently too high. This leads to a simulated annual cycle of

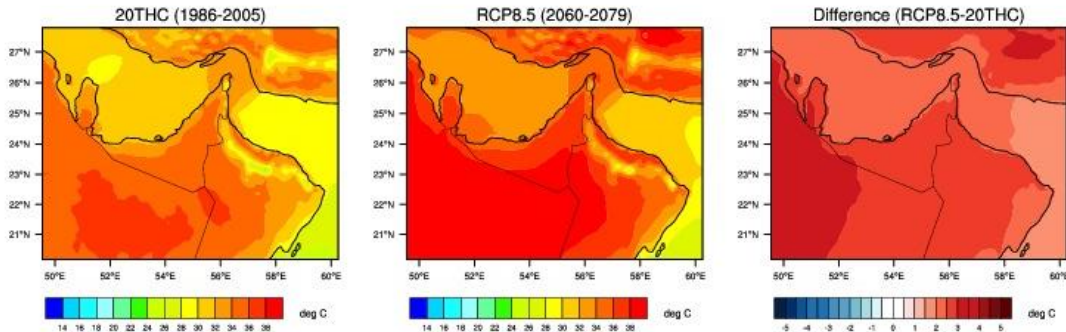
precipitation that is more strongly bimodal than observed, peaking in November/December and again in February/March.

The future climate as projected by the CCSM4 model shows generally warmer and wetter conditions throughout the Arabian Peninsula, although with fairly complex patterns of change, particularly with respect to precipitation. Figure S2 shows average future temperature increases are unanimous across the plotted domain, on the order of 2°-3°C over land areas, with increases slightly smaller over many coastal areas. These changes are consistent across winter and summer. The annual cycle of 2-m air temperature for the WRF simulations for 2060-2079 for five cities in UAE are projected to statistically significantly increase ( $p < 0.01$ ) in all months.

### Average DJF Temperature



### Average JJA Temperature

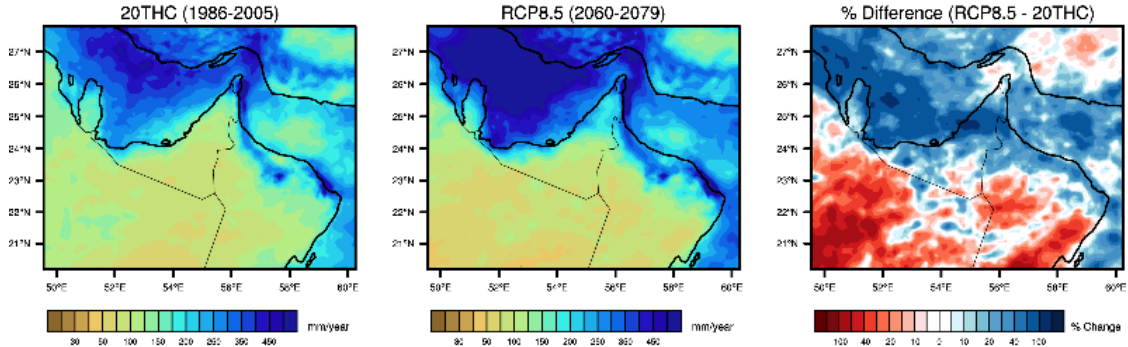


**Figure S2. Average DJF (top) and JJA (bottom) 2-m Air Temperature (°C), for 20THC (left), RCP 8.5 (center), and the difference (RCP 8.5 minus 20THC; right) for Domain D3.**

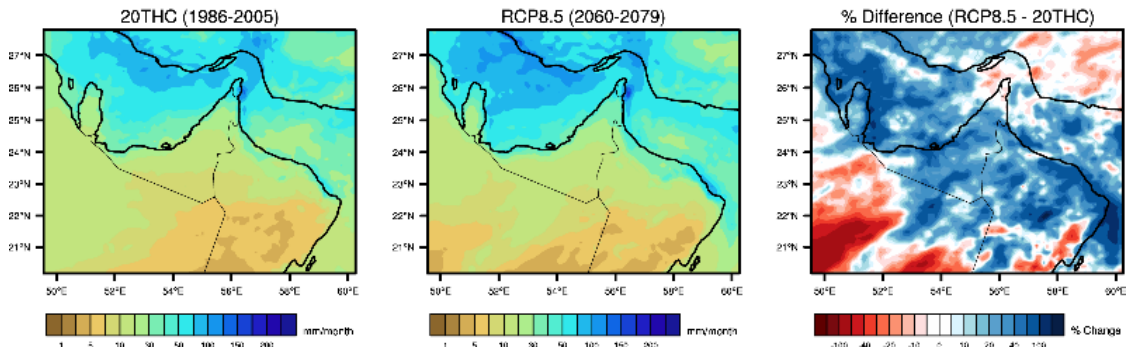
Figure S3 shows the projected rainfall amounts for 20THC (left column), RCP8.5 (center column), and the percentage difference (right column), averaged annually (top row), winter (December-January-February, middle row), and summer (June-July-August, bottom row). In total (top row), rainfall is projected to increase over much of the UAE, the Hajar Mountains, and Qatar. Increases of 50-100% from current amounts are projected for portions Dubai, Sharjah, and northern Abu Dhabi emirates, with increases averaging around 25% over surrounding regions. Increases are also projected over the Arabian Gulf and Gulf of Oman. Decreasing rainfall is projected over much of Oman and eastern Saudi Arabia. Winter (DJF) is

the dominant season for rainfall across the region (middle row), and the projected rainfall increases over the Arabian Gulf and north of the Hajar Mountains primarily occur during this season. Interestingly, during the dry summer season, rainfall increases over much of the UAE are larger than during the wetter winter season, in both absolute value and percentage change. The rainfall increases over the Hajar Mountains and the eastern UAE primarily occur during summer as well. The annual decreases over much of Oman and eastern Saudi Arabia occur during winter and spring (March-April-May). Larger amounts of rainfall occur during comparatively fewer rainfall events than currently observed. Precipitation results should be interpreted with caution, as the future changes are statistically insignificant or only weakly significant during some winter months ( $p < 0.10$ ), suggesting a great deal of noise in the signal. One reason for this low skill in the projection of the change in future precipitation is the existence of some large, anomalous events in the CCSM4 forcing, including cyclones that pass across the region, with heavy precipitation. The WRF model captures these events too.

## Average Annual Rainfall



## Average DJF Rainfall



## Average JJA Rainfall

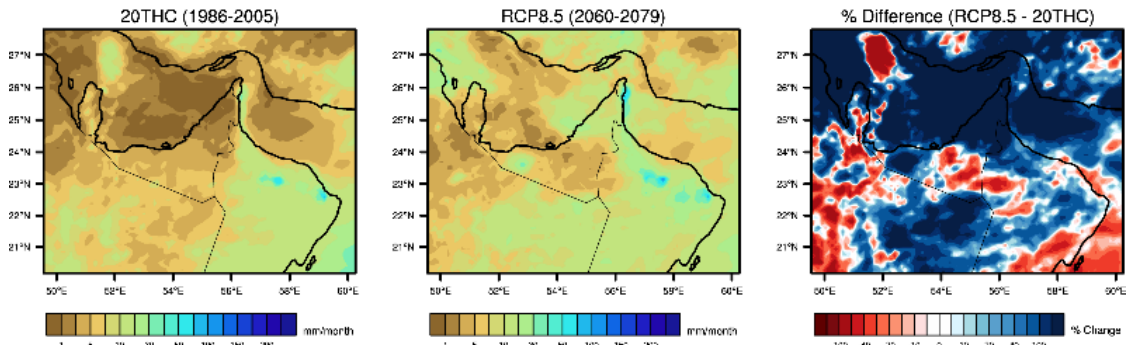


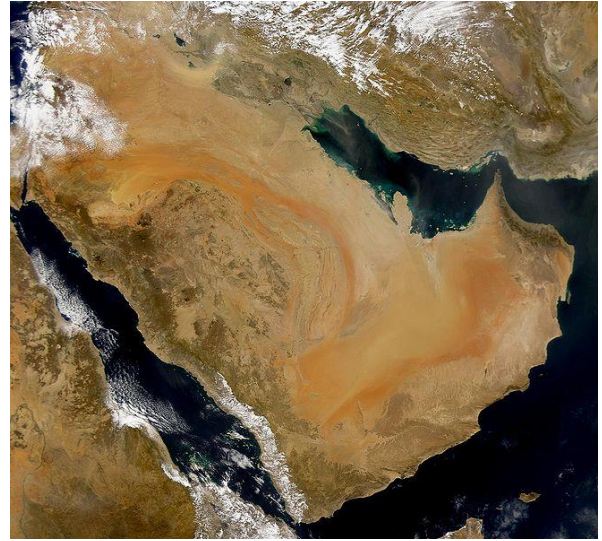
Figure E3. Current and future seasonal rainfall from the 12-km domain. Projections show a complex pattern of increased rainfall.



## 1. Background

The United Arab Emirates (UAE) is situated within the broader Arabian Peninsula region, sharing this large desert landscape with its neighbors that include Kuwait, Bahrain, Qatar, Oman, Yemen, and Saudi Arabia on the Peninsula. The island nation of Bahrain lies off the east coast of the Peninsula, while Iran is situated across and to the north of the Persian Gulf, which has a dramatic influence on the climate of the region. The region is characterized as hyper-arid and has coped with high average temperatures and low rainfall over recorded history. The arid climate means precipitation is typically less than 100 mm/year with a very high potential evaporation rate of 2 to 3 m/yr; and localized groundwater recharge with very low rates. The Arabian Gulf is extensively shallow, especially around the coast of the United Arab Emirates, where is often less than 20 m deep. The tropical climate and the surrounding greater deserts of the region influence the circulation and temperatures of Gulf water. The Shamal winds blow predominantly from a north-northwest direction during the summer, but exert a year-round influence, with seasonal fluctuations but are seldom strong and rarely reaches gale force.

**Figure 1. Looking over the Arabian Peninsula, the Arabian Sea, the Arabian Gulf, and the Red Sea.**



### 1.1 The Climate of the Region

The region is characterized by extremely high temperatures especially in the summer, while there is a strong north-south winter time temperature gradient. Rainfall is sparse throughout the region, with most occurring as short duration events between November and April, with higher amounts in the northeast. Surprisingly, the tall topographic relief of the Oman Mountains provides an environment to trigger summertime convective thunderstorms, providing opportunity for groundwater recharge wadi alluvium.



The Peninsula's low elevation and proximity to the Arabian Gulf means that coastal regions, especially the UAE, are quite humid. Thunderstorms and fog are rare throughout the region, although more prevalent in the wintertime along the UAE coast due to its position, with dust storms and haze occurring frequently in summer.

At roughly 24° North latitude, there is a strong summer/winter contrast in temperature, where summertime highs can reach 50°C in some places, and wintertime lows can be below freezing in the Oman Mountains. The bulk of precipitation occurs in the winter season (December to March), as Troughs, depressions and the occasional front, move through the region from the west and northwest, resulting in large-scale systems that provide significant rainfall. During strong frontal conditions, rainfall can be experienced throughout the country but reaches a peak over the mountains due to additional uplift as airflow is forced over the mountains. Often times these systems have embedded convective elements or even isolated convective cells as the frontal system passes through the region. Strong systems with convective instability occur infrequently, perhaps once or twice a year, while weaker systems occur much more often, resulting in several days of cloud cover and light rain or drizzle. Year-to-year variability of rainfall over the UAE is dramatic, with the standard deviation of annual precipitation larger than the mean. While rainfall can occur throughout the county, it is only over the Oman Mountain region where it is significant enough to yield local, economically viable water resources.



**Figure 2. Looking east towards the Oman Mountains in the Abu Dhabi Emirate**

Wintertime rainfall dominates, but convective rainfall over the Oman Mountains during the summer season is a phenomenon that is widely known to local meteorologists but is not described adequately in climatological studies. During the summer, the UAE region is under the influence of upper level easterly to northeasterly flow associated with the tropical easterly belt, enhanced by the thermal low over the sub-Asian continent. This circulation can provide some moisture from the Arabian Sea. However, the flow at low levels is often from the northwest during the daytime on the UAE side of the mountains due to a sea breeze circulation, forced by surface temperature differences between the desert and the Arabian Gulf. The mountains often initiate convection under these conditions, depending on the wind flow and the thermodynamic profile of the atmosphere. Relatively small changes in the wind flow and thermodynamic structure can result in large changes in cloud development.

## 1.2 Motivation, Context, Goals and Objectives

Information and data from this regional climate modeling study will serve the Climate Change Impacts, Vulnerability and Adaptation Assessment Activities for the Abu Dhabi Environment

Agency, as well as organizations across the broader Arabian Peninsula. For example, climate and hydrometeorological data will be used to explore questions surrounding groundwater recharge. There are not reliable, perennial surface water sources and trans-boundary waters are shared with Saudi Arabia and the Sultanate of Oman, which will be addressed by Activity #11 Transboundary Groundwater Management for the Arabian Gulf Countries. Activity #7 (Water Resources of the United Arab Emirates) and Activity #4 (Sustainability and Resilience in the Al Ain Area) will also make use of the regional climate model data to explore groundwater recharge and water demand questions.

The arid climate of the UAE is favorable to renewable energy prospects, especially solar and wind; although changes in wind-patterns, cloudiness, and changes in aerosol concentrations due to industrial activity or dust from the vast Arabian Desert could impact these resources. The Regional Climate study helps our understanding of the potential impacts of climate change and variability on terrestrial ecosystems (Activity #13, “Key terrestrial ecosystems and species”) and human health related impacts of climate (Activity #6, “Public health and greenhouse gases”). Respiratory and vector borne diseases often have a strong climate link. Projections of future climate change will provide insights into the vulnerability of these sectors and potential adaptation options.

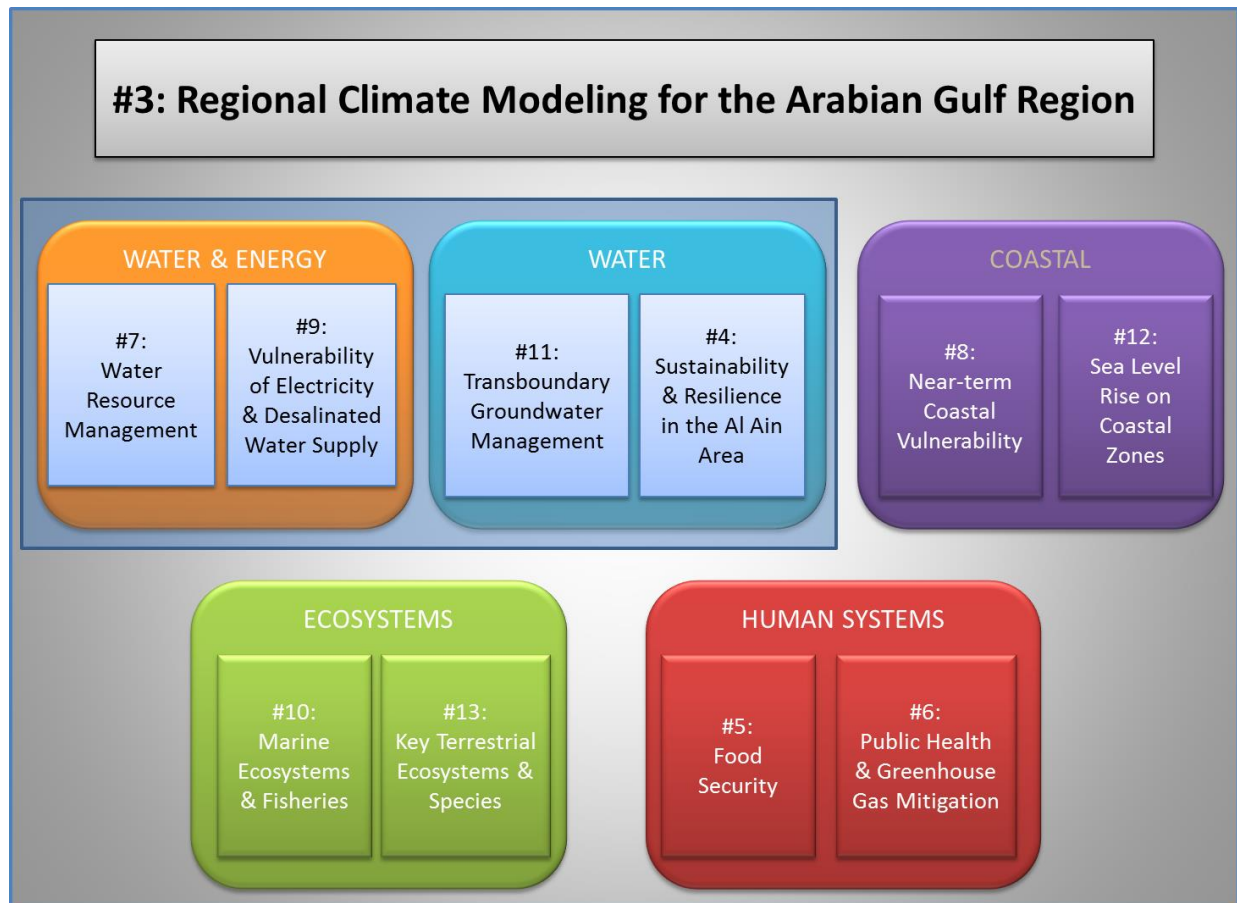


Figure 3. Overview of Concept Proposals and the representation of their inter-connectedness.


This goal of this Regional Climate Modeling Activity was to develop projections of regional climate for the Arabian Peninsula at fine spatial and temporal scale, that reflect the large-scale features and temporal trends from Global Climate Model (GCM) simulations based on the Intergovernmental Panel on Climate Change (IPCC) 5<sup>th</sup> Assessment Report (AR5). To achieve this, a regional climate model (RCM), NCAR's Weather Research Forecast or WRF, was deployed that dynamically downscaled the climate of the Arabian Peninsula using GCM data for lateral boundary conditions. Improved topographic representation across the domain reflects the taller topographic features of the region, which potentially increases and redistributes precipitation due to enhanced lifting. The taller topography also provides a cooler environment for precipitation over places like the Oman Mountains as compared to smoothed topography, which will not resolve warm season convection. The data can be used in support of the other climate change impact, vulnerability and adaptation assessments.

Global Climate Model (GCMs) runs from the 4<sup>th</sup> and 5<sup>th</sup> Inter Governmental Panel on Climate Change (IPCC) Assessments (AR4 and AR5) indicate substantial changes in the climate of the Arabian Peninsula. However, results from these GCM projections summarized in the IPCC reports shows that these projections typically performed poorly in regions of complex terrain due to smoother terrain representation and in those areas that are heavily influenced by local phenomena such as Sea Surface Temperature anomalies. The climate of the UAE and the Arabian Peninsula is, in particular, driven by steep temperature gradients from the Arabian Gulf, the Arabian Desert, and the Oman Mountains, so climate assessments in this region using global models are particularly uncertain. Therefore, it is critical to examine climate impacts in this region using higher resolution models that can more realistically represent local to regional meteorological dynamics, such as orographic precipitation, land-ocean wind breezes and circulations, surface heating and evaporation, on-shore and off-shore wind patterns, etc. This study has achieved this objective by deploying the WRF model on the NCAR-Wyoming Supercomputer (NWSC) or "Yellowstone", which is a 1.5-petaflops high-performance IBM iDataPlex cluster, which features 72,576 Intel Sandy Bridge processors and 144.6 TB of memory. For this project, we used nearly one million core hours of processor time and we estimate that on a modern, quad core laptop, the experiment run for this study would take nearly 30 years to complete.


It should be noted that the data archive from this regional climate modeling experiment is quite large. We estimate a data archive of nearly 110 Terra-Bytes. Because of this large size, we believe it makes more sense to demonstrate the datasets that can be developed, and then work with our stakeholders to derive specific datasets that they might need for their studies. In this way, we hope other researchers can identify specific derived products that they might find useful, and that such a process would provide an opportunity to influence and/or directly affect subsequent research activities. Also, we will be making a web-based data explorer, where interested users will be able to access daily data from the RCM experiments, for precipitation, air temperature, humidity, wind speeds, and other variables.


### 1.3 Research team

**An international team of experts was assembled to undertake the specific research activities associated with this sub-project.** The project team consists of atmospheric scientists and climate impact specialists with proven research records in regional atmospheric modeling, data analysis and synthesis, and the use of climate projections in impact and adaptation research. The structure of the project team consists of a Principal Investigator (PI) and a Research Team (RT). An overview of individual members of the project team is provided in the bullets below.

- *Principal Investigator:* David Yates has served as the PI of the Regional Atmospheric Modeling sub-project. David is a Scientist in the Research Applications Laboratory at NCAR and his role has been directing the regional climate modeling experiments and providing guidance and insight to the Project Scientists on needs and requirements. He was responsible for keeping the project on time and on budget, providing monthly reports, producing the final report, and generating user product datasets. 

- *Research Team:* The RT consisted of several experts that brought expertise on various dimensions of the sub-project, as briefly described below.

- ✓ *Dr. Dan Steinhoff.* Dan is a Project Scientist in the Research Applications Laboratory at National Center for Atmospheric Research (NCAR), Boulder Colorado. He has ten years of experience in numerical weather prediction, regional-scale meteorology, and satellite data processing and analysis. His current research interests span regional-scale climate modeling, climate and infectious disease, and defense-related meteorological applications. He served as the primary WRF modeler. 

- ✓ *Dr. Andrew Monaghan.* Andy is an atmospheric scientist at NCAR, where his research interests include the use WRF and other model-based techniques to study climate-sensitive health and disease issues. Dr. Monaghan has a BS degree in civil engineering from the University of Alaska-Fairbanks, and Masters and PhD degrees in atmospheric sciences from The Ohio State University. 

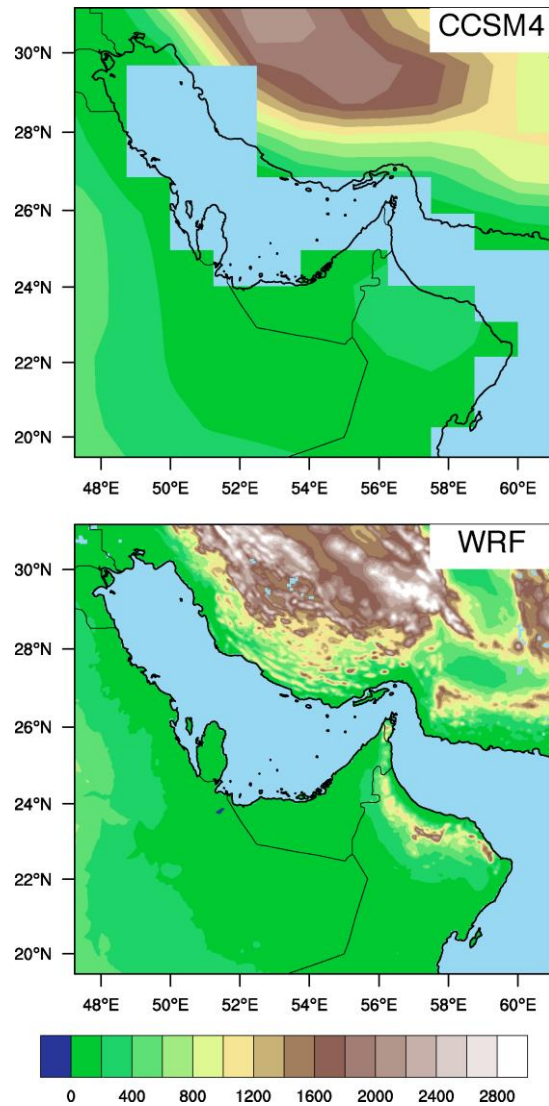


## 2. Overview of Experiment and Methodological Approach

WRF climate simulations were performed over both historical and future periods, and derive their initial and boundary conditions from a coupled, atmosphere-ocean global climate model or AOGCM. AOGCM's represent the most readily available sources of multi-decadal climate data for present-day and future applications, respectively. However, for many applications, global datasets do not have adequate spatial or temporal resolution to resolve the local or regional aspects of weather and climate. Therefore, regional climate models (RCMs) are frequently employed to dynamically interpolate these comparatively coarse resolution global datasets to smaller geographic regions, typically on a case-by-case basis. The RCM thus provides data of finer spatial and temporal resolution that is needed by the adaptation community. This process of transforming coarse scale, GCM data to the fine scale is commonly referred to as *downscaling*.

The WRF climate simulations in this study derive their initial and boundary conditions from the NCAR AOGCM- Version 4 of the Community Climate System Model (CCSM4; Gent et al. 2009). Figure 2 compares the terrain from the CCSM4 AOGCM, which is approximately 100 km in horizontal extent, to that of the WRF 4-km domain.

It is clear that CCSM4, with a spatial resolution of 0.9 degrees latitude x 1.25 degrees longitude (approximately 100 km), cannot adequately resolve the topography of the Oman mountains and other important orography in the region compared to WRF, demonstrating the necessity of performing the WRF dynamical downscaling simulations in order to provide a dataset that is appropriate for assessing climate change in the region.



**Figure 4. Terrain height (m, color scale at bottom) and land/sea mask for CCSM4 (top) and 4-km WRF (bottom). Actual coastlines and political boundaries shown in black.**



The purpose of performing the AOGCM-driven WRF climate simulations for the historical period is to 1) generate a dataset that can be used to validate the AOGCM-driven WRF simulations against the reanalysis-driven WRF benchmark simulations described above for some common historical period, and 2) provide a baseline dataset against which future AOGCM-driven WRF climate simulations can be assessed. The purpose of performing the AOGCM-driven WRF climate simulations for the future period is to provide a projection for the future state of the atmosphere in some latter portion of the 21st century.

## 2.1 The Global Climate Model Context

The primary input to RCMs is coarse-scale, gridded meteorological forcing data from Global Climate Model (GCM) archives. Each climate modeling center that develops, tests, and runs GCMs, also archives their model results according to strict standards through a Climate Model Inter-comparison (CMIP) process. This standardization affords researchers the opportunity to conduct regional climate modeling experiments by obtaining the archives from high bandwidth data servers. The datasets are 3-dimensional in space, are on a 6-hourly timestep, cover the entire globe, and include variables such as wind, temperature, pressure, and others. For example, the Earth System Grid (ESG) provides a distributed archive of GCM results from the primary modeling centers around the world, such as NCAR, the UK Meteorological office (UKMet), etc., where modelers obtain archives of data from Global Models such as the European Center for Medium Range Forecast (ECMWF), the ERA-Interm Reanalysis (ERA-Interm) datasets, the NCAR Climate and Earth System Model (CESM), etc.

The most comprehensive projections of future global climate conditions are provided by atmosphere-ocean general circulation models (AOGCMs). Problematically for those involved in climate change adaptation planning, outputs from AOGCMs are typically available at spatial scales of 100 kilometers or more. Furthermore, different AOGCMs run under the same greenhouse gas emissions forcing scenario can produce profoundly different projections of temperature and precipitation change, particularly at the regional scale (see the IPCC 2013 report for a comprehensive discussion of AOGCM predictions). Global climate models (GCMs) are mathematical representations of the behavior of the Earth's climate system through time. Each model couples the ocean, the atmosphere, and the land and ice surfaces, and climate models have increased in complexity as computational power has increased. Recent integrated climate models simulations, done for the IPCC 2007 Report, were run at higher spatial resolution than earlier models and, due to improved physical understanding, incorporated more accurately complex physical processes such as cloud physics.

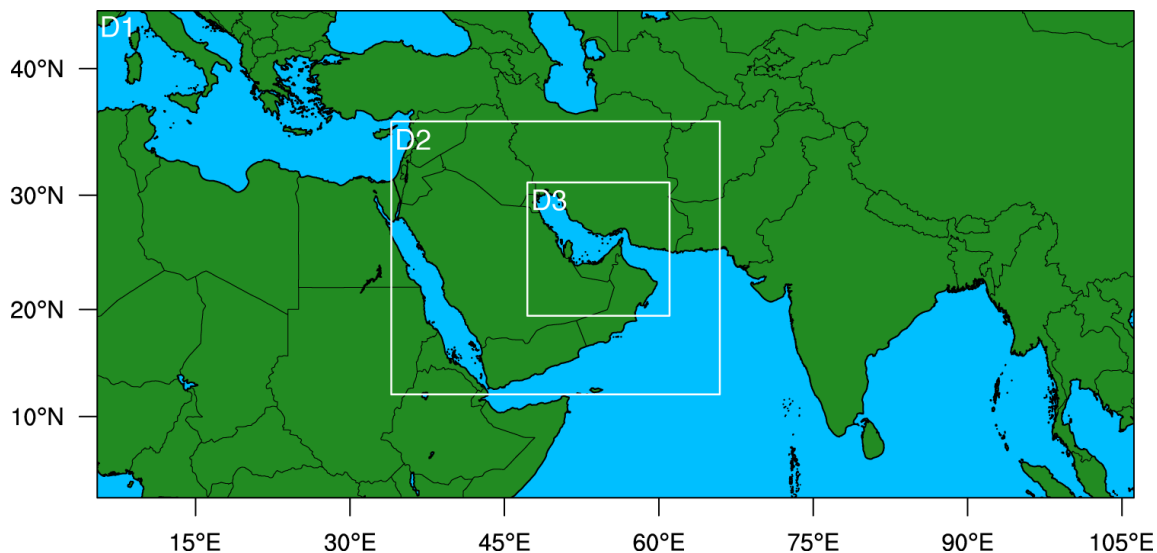
***WRF-** The Regional Climate Model and its Configuration To quantify 21st century climate change over the UAE and Arabian Gulf region, we performed simulations using version 3.5.1 of the Weather Research and Forecasting Model (WRF, Skamarock et al. 2008). WRF is a fully compressible conservative-form nonhydrostatic atmospheric model with demonstrated ability for resolving small-scale phenomena and clouds (Skamarock and Klemp 2008). Here, WRF is employed to dynamically downscale climate fields from a comparatively coarse-scale gridded global domain to a comparatively fine-scale regional domain that is relevant for assessing*

*climate change impacts at regional-to-local scales. The WRF computational domains are shown in Figure 1. The outer domain with a grid spacing of 36-km resolution (“D1”) covers much of the eastern hemisphere. Nested inside the 36-km domain is a 12-km domain (“D2”) covering the Arabian Gulf region. The innermost 4-km nested domain (“D3”) covers the UAE and vicinity.*

**Domain 1:** 36 km resolution, with 283 (E-W) x 133 (N-S) grid cells. We have tested domain 1, and believe that a larger domain, which extends eastward, beyond the Himalayas, will help to avoid computation problems on the model boundaries.

**Domain 2:** 12 km resolution, with 229 (E-W) x 223 (N-S) grid cells. This is another extensive domain, which extends northward to cover mountain ranges in Iran.

**Domain 3:** 4 km resolution, with 289 (E-W) x 196 (N-S) grid cells. This is the highest resolution domain (and computationally the most expensive). The domain covers UAE and surrounding region. See Figure for details.



**Figure 5. Domains used in WRF simulations.**

The WRF simulations feature 40 vertical levels from the surface to 10 hPa (about 30 km above the surface). The WRF simulations are reinitialized every eight days, and each eight-day period is preceded by a 12-hour period that allows the WRF hydrological fields to spin up, and which are subsequently discarded. Throughout the simulations, four-dimensional data assimilation (FDDA, Stauffer and Seaman 1994) -- i.e., “grid nudging” -- is employed on the 36-km domain to keep the model solution from diverging from the large-scale global boundary conditions, which are described in detail below. Physical parameterization schemes, which simulate the sub-grid scale processes in WRF empirically, include the Lin microphysics scheme, the RRTM longwave radiation scheme, the Dudhia shortwave scheme, the MM5

surface layer scheme, the Noah land surface model, the YSU PBL scheme, and the Grell-Devenyi convective scheme (36-km and 12-km domains only).

These parameterizations are chosen because they yielded optimal WRF performance over the UAE when compared to in-situ precipitation and temperature fields for the July and December 1995 case study periods. The global domains providing the initial and lateral boundary conditions for the WRF dynamical downscaling simulations come from two sources depending on whether they are “benchmark” simulations or “climate” simulations, which are described next

### 3. WRF Simulations of Current and Future Climate

The study included continuous simulations of the 12-km and 36-km domains. The 4-km domain was run over shorter time periods, simply because those runs were very expensive.

Figure 6 summarizes the experiment, with the following simulations performed:

1. A 30-year ERA-Interim driven WRF benchmark simulation for the historical period spanning 1981-2010 (36- and 12-km domains)
2. A 20-year bias-corrected-CCSM4-driven WRF climate simulation for the historical period spanning 1986-2005 (36- and 12-km domains). The 4-km domain was turned on for the 1990-1999 sub-period.
3. A 20-year bias-corrected-CCSM4-driven WRF climate simulation for the RCP4.5 period spanning 2060-2079 (36- and 12-km domains)
4. A 20-year bias-corrected-CCSM4-driven WRF climate simulation for the RCP8.5 period spanning 2060-2079 (36- and 12-km domains).
5. The 4-km domain was turned on for 10 years forced by bias-corrected CCSM4 boundaries in the contemporary period 1990-2000 and the future period, 2065 to 2075.

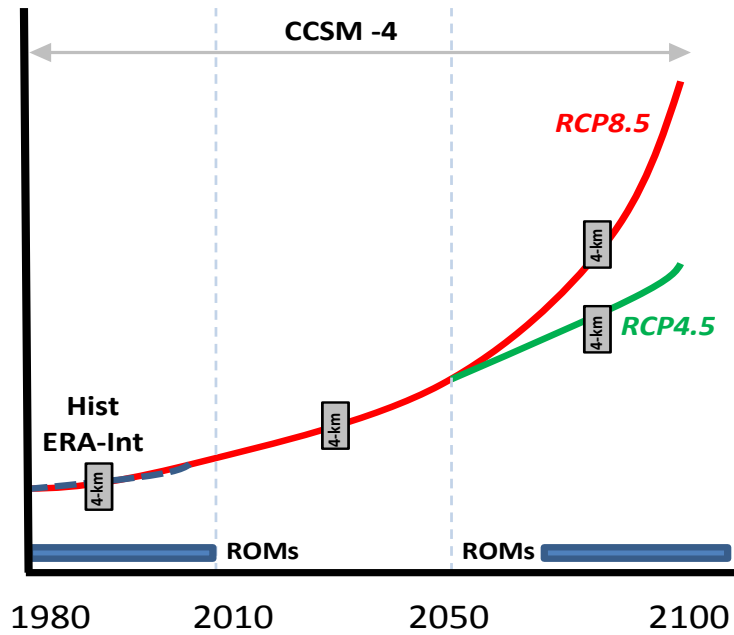


Figure 6. *The Experimental Design. WRF was run for 20 and 10 years for the contemporary period and the future period at 12 and 36 km; and 4-km, respectively.*

### 3.1 WRF Climate Simulations with ERA-Interim

WRF benchmark simulations were performed over a historical period and were used to estimate the true state of the atmosphere. The benchmark simulations in this study derive their initial and boundary conditions from the European Centre for Medium-Range Weather Forecasting (ECMWF) Interim Reanalysis (ERA-Interim; Dee et al. 2011). ERA-Interim is considered to be the most accurate atmospheric reanalysis available at the present time (e.g., Lorenz and Kunstmann 2010). The ERA-Interim fields employed here have  $\sim 0.7^\circ$  grid spacing on 38 vertical levels. Sea surface temperature (SST) data at the lower oceanic boundaries of these benchmark simulations are from version 2 of the National Oceanic and Atmospheric Administration (NOAA) Optimum Interpolation (OISST) 0.25 degree product (Reynolds et al. 2007).

Figure 7 and Figure 8 demonstrate from the simulations with WRF driven by the ERA-Interim reanalysis data. These simulations represent real meteorological events in the summer and winter of 1995, respectively; where simulated rainfall is compared to measured rainfall across the UAE. In December, positive biases surround the coastal areas, while the largest negative biases are again clustered along the large rainfall gradients over the steep terrain.

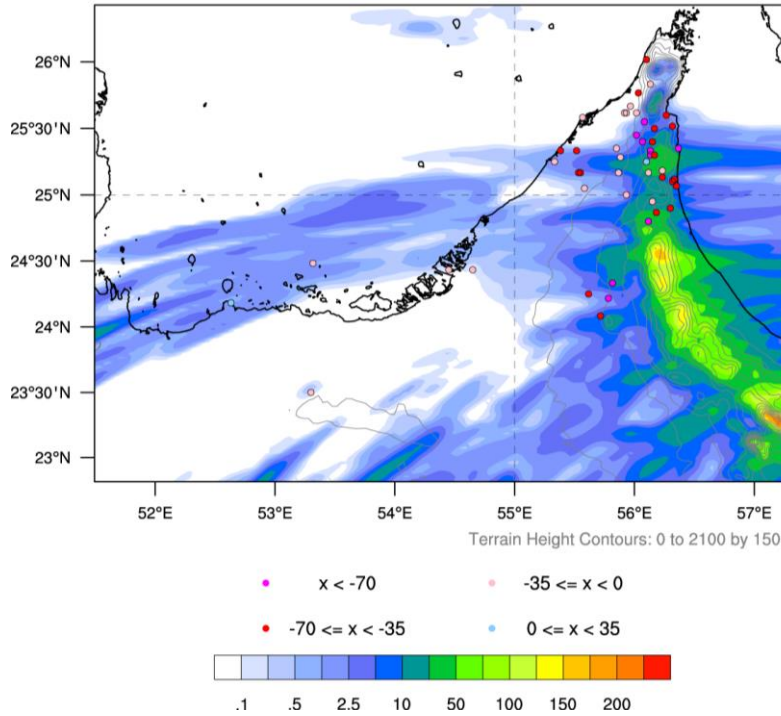


Figure 7. WRF rainfall biases (color-coded dots), WRF rainfall (mm, color shading), and WRF terrain height (gray contours) for July 1995 for subset of domain in Fig. 1.

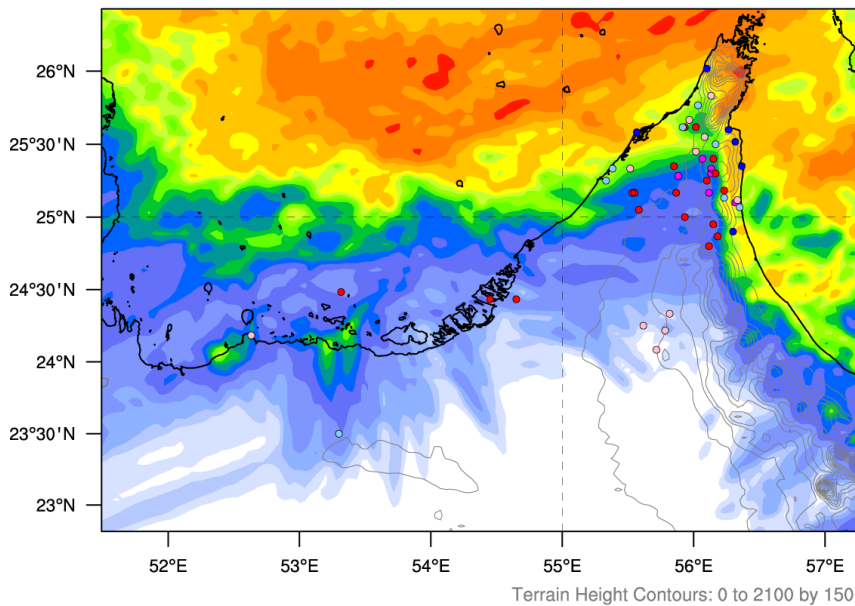


Figure 8. Same as (a) except for December 1995.

Figure 9 shows daily rainfall tendencies for observed (blue) and WRF (red) for some sample locations for December 1995. WRF broadly follows the observed accumulations throughout the month, but often with different magnitudes. Results for July 1995 not shown – all rainfall occurred July 22-26, which WRF simulated but with greatly underestimated amounts.



**Figure 9. Daily rainfall tendencies for selected locations for December 1995. Observed tendencies in blue and WRF tendencies in red.**

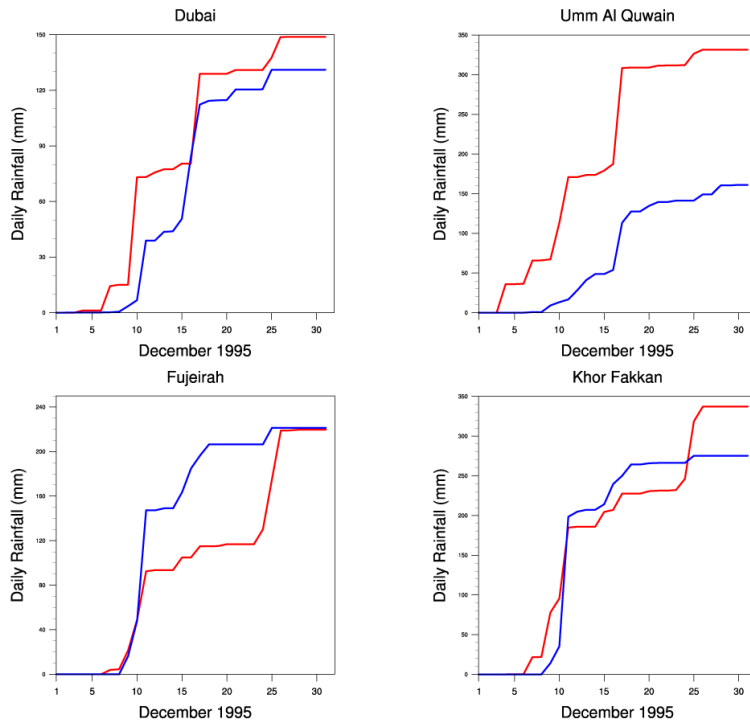
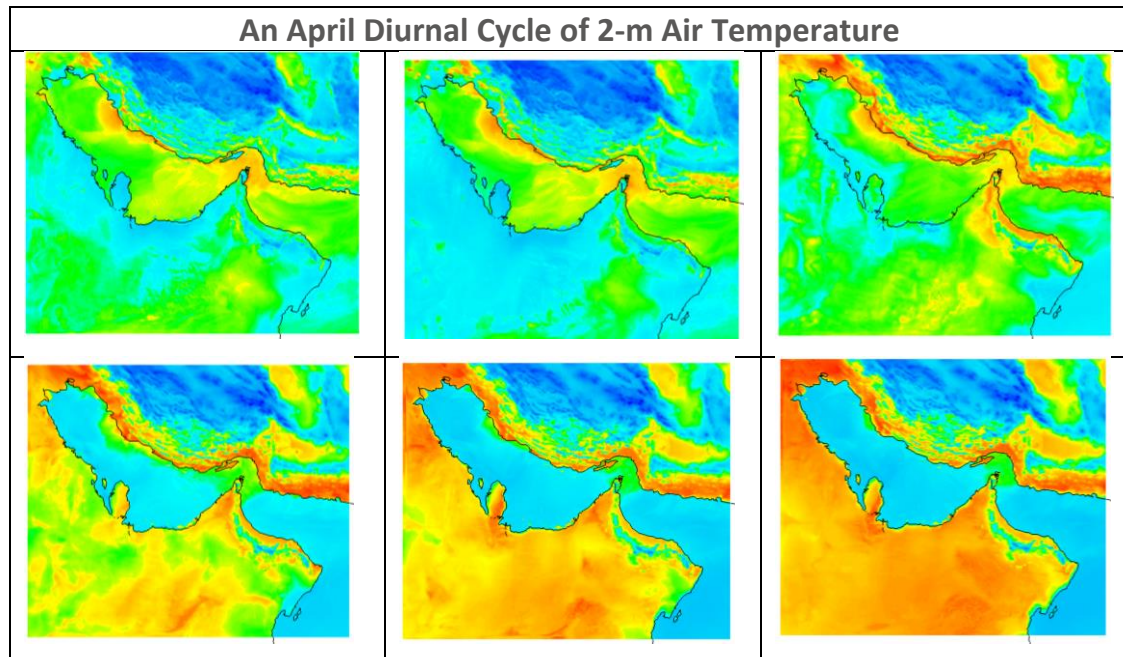


Figure 10 shows a diurnal cycle of surface temperature for a day in April in 1995, when WRF is forced with the ERA-Interim data. Note that at 4-km resolution, the WRF model is able to capture important temperature gradients along coastlines and throughout the Oman Mountains.



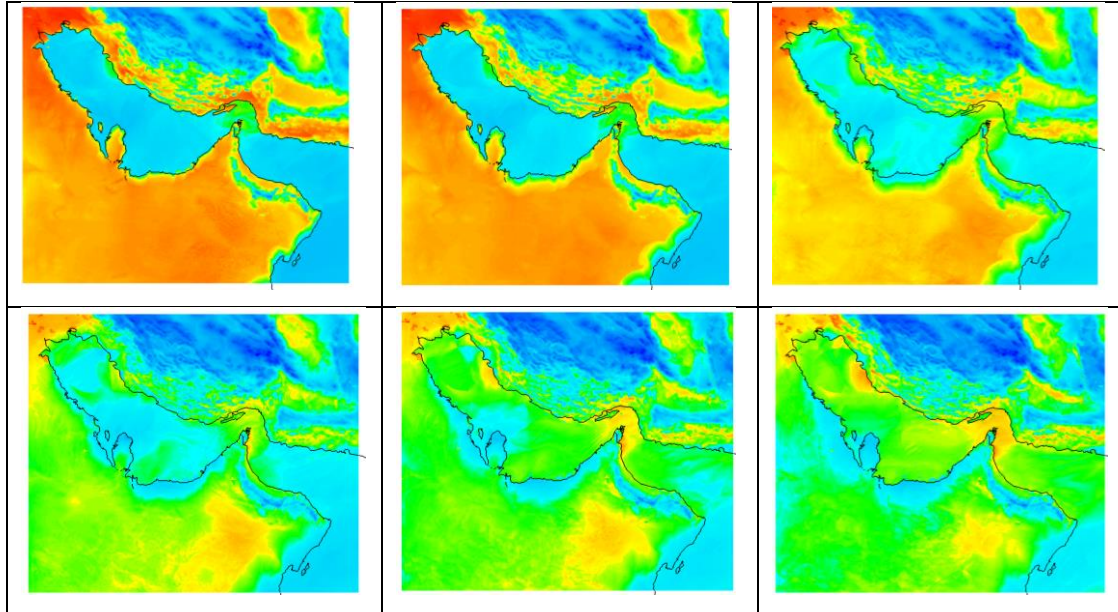


Figure 10. A sample case of diurnal cycle of 2-m air temperature from D03, which is the 4-km domain. Upper left 00:00 Local, 02:00 local upper middle, 04:00 upper right; and 22:00 low right.

We ran sensitivity simulations with WRF to improve upon the rainfall estimates shown above. These simulations involve modifying model features such as microphysics parameterization schemes, planetary boundary layer parameterization schemes, the use of a cumulus parameterization scheme, input datasets, and model grid spacing. We performed a similar analysis on each of the sensitivity simulations as we did above to find a “best” model setup. Note that other model configurations could have been chosen that would lead to different states of model performance.

## 3.2 WRF climate simulations with CCSM4 (Boundary Forcing)

The CCSM4 simulations that provide the initial and boundary conditions for the WRF climate simulations were performed in support of the Coupled Model Intercomparison Experiment Phase 5 (CMIP5; Taylor et al., 2012) and the Fifth Assessment Report of the Intergovernmental on Climate Change (IPCC 2013). CCSM4 ranks at the top of all CMIP5 AOGCMs in its ability to simulate observed temperature and rainfall globally (Knutti et al. 2013). Model fields were obtained from NCAR’s ESG portal (<https://www.earthsystemgrid.org/>) and are also available from the Earth System Grid - Program for Climate Model Diagnosis and Intercomparison (ESG-PCMDI) gateway at Lawrence Livermore National Laboratory, <http://pcmdi3.llnl.gov/>. The CCSM4 ensemble member chosen was the *r6i1p1* with an *f09\_g16* or *0.9x1.25\_gx1v6* resolution. This resolution translates into a distance of about 100 km along a latitudinal transect and 125 kilometers along a longitudinal transect across the Arabian Peninsula.

The CMIP5 model scenarios used in this study include a historical simulation and two future projections. The historical simulation was forced by observed natural and anthropogenic atmospheric composition changes spanning 1861-2005. The future projections are the Representative Concentration Pathway (RCP; Moss et al. 2010) 4.5 and 8.5 scenarios, which span 2006-2100. RCP4.5 is a low-to-moderate emissions scenario with GHG radiative forcing reaching 4.5 W m<sup>-2</sup> near 2100. It represents a trajectory that may be plausible (and desirable) if, for instance, GHG emissions pricing were introduced in order to limit radiative forcing (Thompson et al. 2011). RCP8.5 is a high-emissions scenario with greenhouse-gas (GHG) radiative forcing reaching 8.5 W m<sup>-2</sup> near 2100. It represents a plausible trajectory if little is done to curb greenhouse gas emissions (Riahi et al. 2011). Ensemble Member #6 of the historical, RCP4.5 and RCP8.5 CCSM simulations was used, as that is the only member that has available at 6-hourly intervals the full three-dimensional fields required to force WRF.

Like all AOGCMs, CCSM4 contains regional-scale biases due to having coarse spatial resolution and a limited representation of some physical processes. Such biases can adversely affect the dynamical downscaling process and contribute to uncertainty. To remedy these biases, it is common to bias correct the climate model output before using it to drive regional-scale models like WRF (e.g., Rasmussen et al. 2011). In this study a recently-developed bias correction method was applied which corrects for the mean bias in the CCSM4 3-dimensional temperature, geopotential height, wind, and humidity fields, as well as the SST, skin

temperature, and soil temperature and moisture fields. Although the bias in the mean state is corrected, the methodology still allows synoptic-scale and climate-scale variability to change in the future as simulated by CCSM4 (Xu and Yang 2012; Done et al. 2013; Bruyère et al. 2013). The bias-corrected CCSM4 output is produced by summing the average 6-hourly annual cycle (the Reynolds averaged mean term) from ERA-Interim (1981-2005) and a 6-hourly perturbation term (the Reynolds averaged eddy term) from CCSM4:

$$CCSM = \overline{CCSM} + CCSM'$$

$$ERAINT = \overline{ERAINT} + ERAINT'$$

$$CCSM_R = \overline{ERAINT} + CCSM'$$

where overbar terms are the mean climatology, primed terms are perturbations from the climatology, and CCSMR is the revised (bias-corrected) CCSM4 output at 6-hourly intervals, which is subsequently used as the initial and boundary conditions for the WRF climate simulations.

### 3.3 Simulated Regional Climate for the Contemporary Period

To place the CCSM4 climate simulations for the Arabian Peninsula in the context of the larger ensemble of GCMs run for the IPCC AR5 assessment, we show the precipitation anomaly for the region for the ensemble mean from more than 15 GCMs. Many of the individual GCMs include multiple runs or ensemble members, run with the same forcing conditions. The “take-home” message from Figure 11 is that the ensemble of all the climate models shows a generally increasing trend of precipitation for the 21<sup>st</sup> century for the Arabian Gulf region, with an upward trend beginning around the year 1980, with the per-day precipitation averaging about 0.38 mm in 1980, and increasing to about 0.43 mm by 2100.

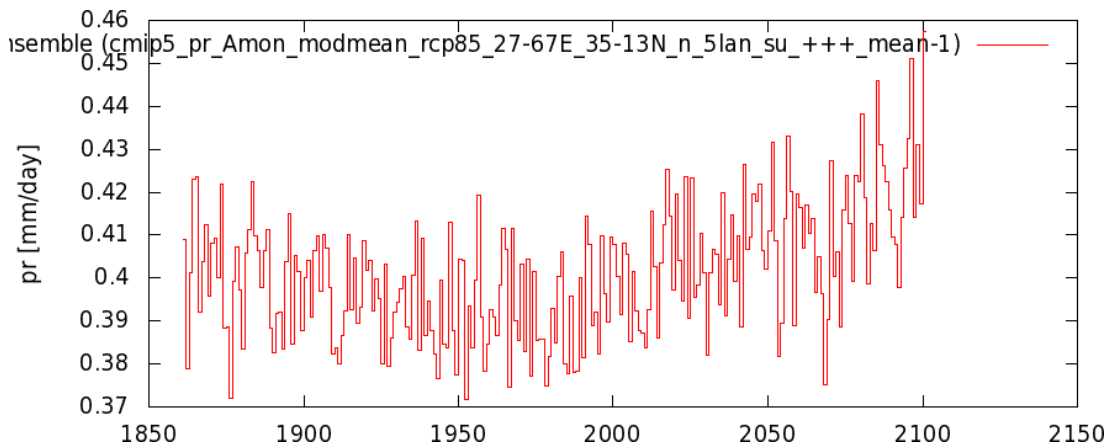
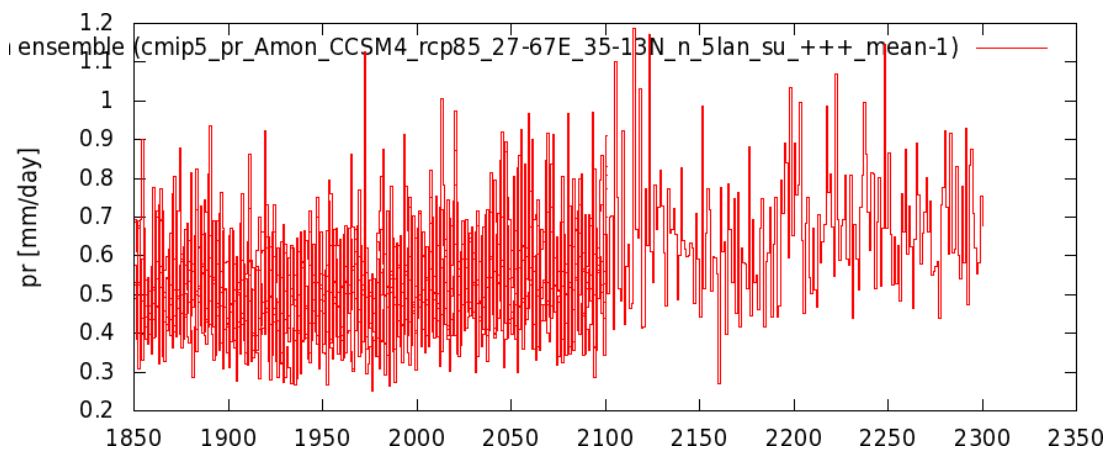


Figure 11. Mean precipitation anomaly from the full suite of GCMs from the IPCC AR5 experiment for the Arabian Peninsula region.



The CCSM4 AR5 simulation has a greater daily precipitation amount for the baseline period (about 0.5 mm/day) when compared to the ensemble mean (about 0.39 mm/day). In similar fashion, the CCSM4 AR5 simulations exhibits an upward precipitation trend beginning in 2000, Regionally, the CCSM4 show a greater increase in precipitation in comparison to the ensemble mean of all the AR5 climate models from an absolute sense, with an increase by 2100 of less than 0.1 mm/day.

Note that the range of the projected change in precipitation from the ensemble mean is about 0.05 mm/day. We conclude from this analysis that the CCSM4 scenario used as the boundary forcing for the WRF model simulates greater precipitation over the 21<sup>st</sup> century for the Arabian Peninsula. The CCSM4 future projection is consistent with the ensemble mean, although the future projection suggests it is one of the “wetter” models for region.



**Figure 12. Projected change in the precipitation anomaly for the CCSM model, which includes multiple ensemble members. Some ensemble members included very long runs past 2100, which extend to 2300.**

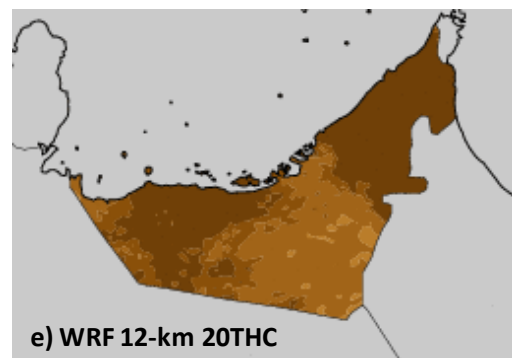
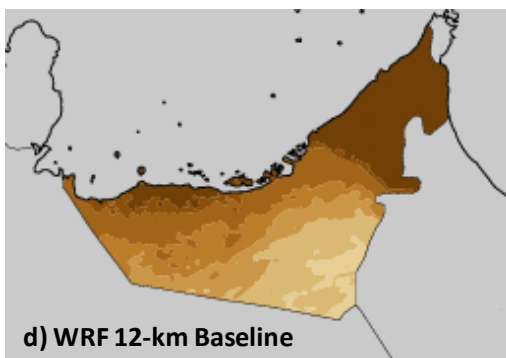
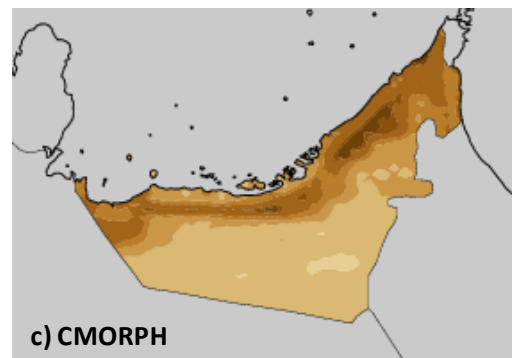
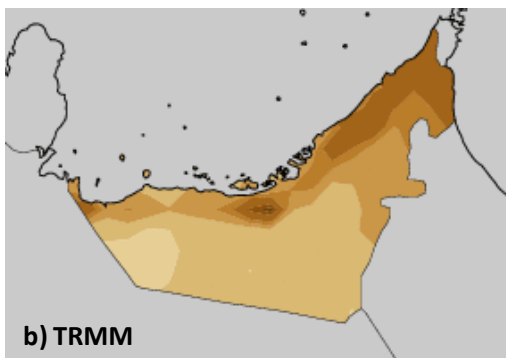
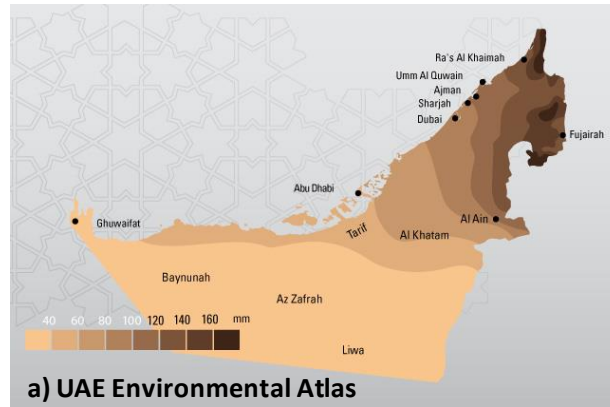
To estimate the projected precipitation changes over the UAE and Arabian Peninsula, WRF simulations were run (using the bias-corrected CCSM4 variables as input) for two time periods: present-day conditions (1986-2005, denoted as “20THC”), and the RCP 8.5 scenario (2060-2079, denoted as “RCP8.5”).

Estimates of long-term annual average precipitation over the UAE from the UAE Environmental atlas, satellites, and WRF simulations are shown in Figure 13. Annual observed precipitation amounts vary from less than 40 mm to more than 160 mm in the northeastern section of the UAE due to the mountainous orography and enhanced exposure to the Indian Ocean. Satellite-based estimates of precipitation (Figure 13. b,c) exhibit patterns and amounts similar to those shown in the UAE atlas, though they suggest that precipitation amounts just inland of the entire Arabian Gulf coast (where there are few observations to confirm) are higher than estimated by the atlas, on the order of the precipitation amounts seen in northeastern UAE. The WRF 12-km baseline simulations driven by ERA-Interim (Figure 13. d) exhibit similar spatial patterns to those seen in the UAE atlas and the satellite-based datasets, though amounts are higher in northeastern UAE. The WRF 12-km, 20THC



simulations driven by the bias-corrected CCSM4 dataset exhibit higher rainfall than in the other datasets, particularly in the western part of the UAE.

From this comparison, it can be seen that the WRF model is capable of representing the spatial patterns precipitation with good skill, although WRF appears to overestimate the magnitudes of rainfall, particularly in eastern portion of the country even when forced with the ERA-Interm baseline. Also, although the CCSM4 forcing model has been bias-corrected to the ERA-Interm Reanalysis dataset, the regional precipitation is greater, which was not surprising given the CCSM4 projection used here was regionally more wet (see Figures 11 and 12).



Annual Rainfall (mm)

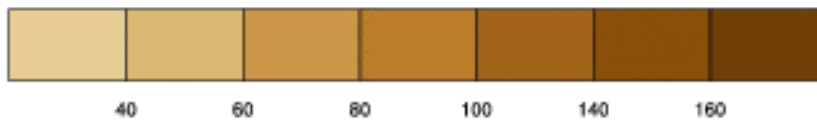


Figure 13. Annual precipitation estimates from a) the UAE Rainfall Atlas, b) NASA's TRMM sensor (~25 km resolution; 1999-2011 average), c) the CPC CMORPH product (~8 km resolution; 2003-2009 average), d) the WRF "Baseline" simulations driven by ERA-Interim (12-km resolution, 1986-2005 average), and e) the WRF 20THC simulations driven by CESM (12-km resolution, 1986-2005 average).

Observations and WRF Baseline and 20THC simulations of the annual cycle of temperature are shown in Figure 14, for five cities in the UAE. The WRF baseline and 20THC simulations

both capture the annual cycle of temperature reasonably well. A cold bias of generally less than 1°C is evident in the spring and early summer months, whereas there is a warm bias of about 3°C evident during the autumn and winter months. The cold-bias may be partly linked to a positive precipitation bias during the autumn winter months (Figure 14), which suggests that the simulations may be cloudier than observed. Interestingly, the observed temperatures for Sharjah and Dubai show summer mean temperature differences of about 2°C, despite the fact that the observations are made at the airports, which are only 20-km apart. It appears that the airports are both a few kilometers inland from the Arabian Gulf coastline, and therefore it is uncertain what would cause this difference. It is possible that heavier urbanization near the Dubai International Airport causes slightly higher temperatures there, although instrument bias and measurement error could also be a contributing factor.

Observations, WRF Baseline and 20THC simulations of the annual cycle of precipitation are shown in Figure 15 for the same five cities. The WRF Baseline and 20THC simulations yield similar results, although winter precipitation is greater in the WRF 20THC simulations. This suggests that the bias-corrected CCSM4 dataset used to drive the WRF 20THC simulations adequately resolves regional weather processes compared to the ERA-Interim dataset used to drive the WRF Baseline simulations. Therefore, any limitations of the WRF 20THC simulations are not likely to be due to the choice of CCSM4 as a driving dataset, with some limitations- most notably winter precipitation.

WRF reasonably captures the magnitude of precipitation during January through October; however during November and December precipitation amounts are consistently too high. This leads to a simulated annual cycle of precipitation that is more strongly bimodal than observed, peaking in November/December and again in February/March. The observed annual cycle is less bimodal (though it is slightly bimodal at Ras al-Kaimah and Fujairah), and peaks in February/March. It is not currently clear why the wet bias exists during November and December, however the large standard deviation of the rainfall amounts during those months suggests that it may be due to a handful of simulated storms that are either stronger than observed, or perhaps track more toward UAE than observed. We also not some strong cyclonic events that propagate from east-to-west, across the Arabian Sea and pass over the UAE.

While large cold-season events do occur -- maximum observed monthly precipitation amounts of 31 mm (Nov), 130 mm (Dec), 109 mm (Jan), 150 mm (Feb), and 155 mm (Mar) have been recorded at Dubai International Airport and generally are attributed to cold season Shamals (northwesterly winds)-- it is likely that WRF produces more heavy precipitation events than are observed. Regardless of the reason, the larger-than-observed precipitation during November and December is the primary reason that simulated annual precipitation amounts shown in Figure 3.4 are too high. Overall, however, the annual cycle and magnitude of precipitation throughout the other ten months is reasonably simulated, suggesting that the model is capturing the primary processes leading to precipitation, and lending confidence that the climate change projections presented in the following section have fidelity.

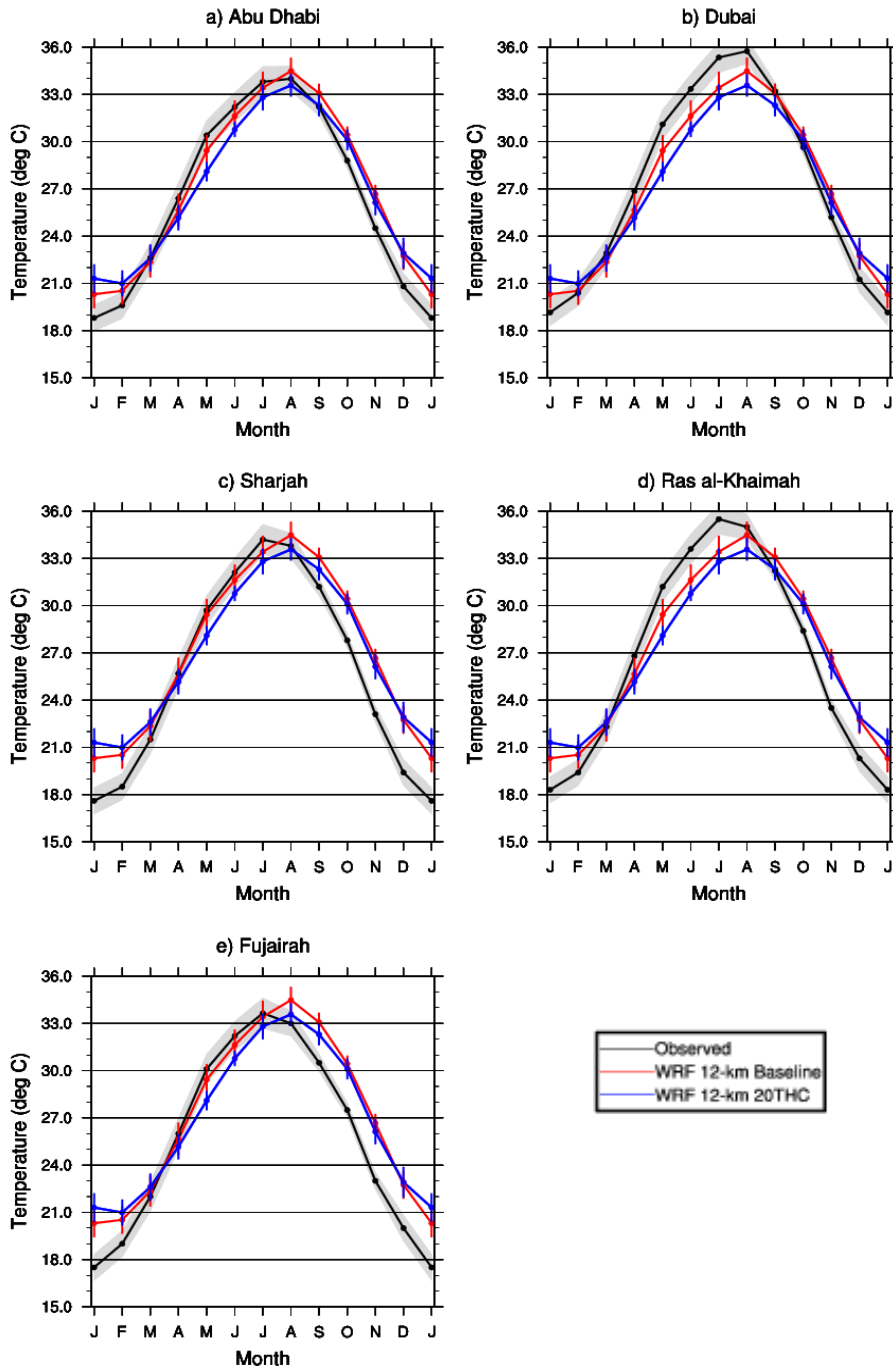


Figure 14. Average monthly observed (various periods) versus modeled (1986-2005) temperature in five UAE cities. Observed temperature records are obtained from the Dubai Meteorological Office (Dubai), the National Oceanic and Atmospheric Administration (Abu Dhabi, Sharja and Ras al-Kaimah), and [www.myweather2.com](http://www.myweather2.com) (Fujairah). Error bars and shading indicate standard deviations of monthly means, with the observed standard deviation values are assumed to be the same as for the WRF 12-km baseline, because data were not available.

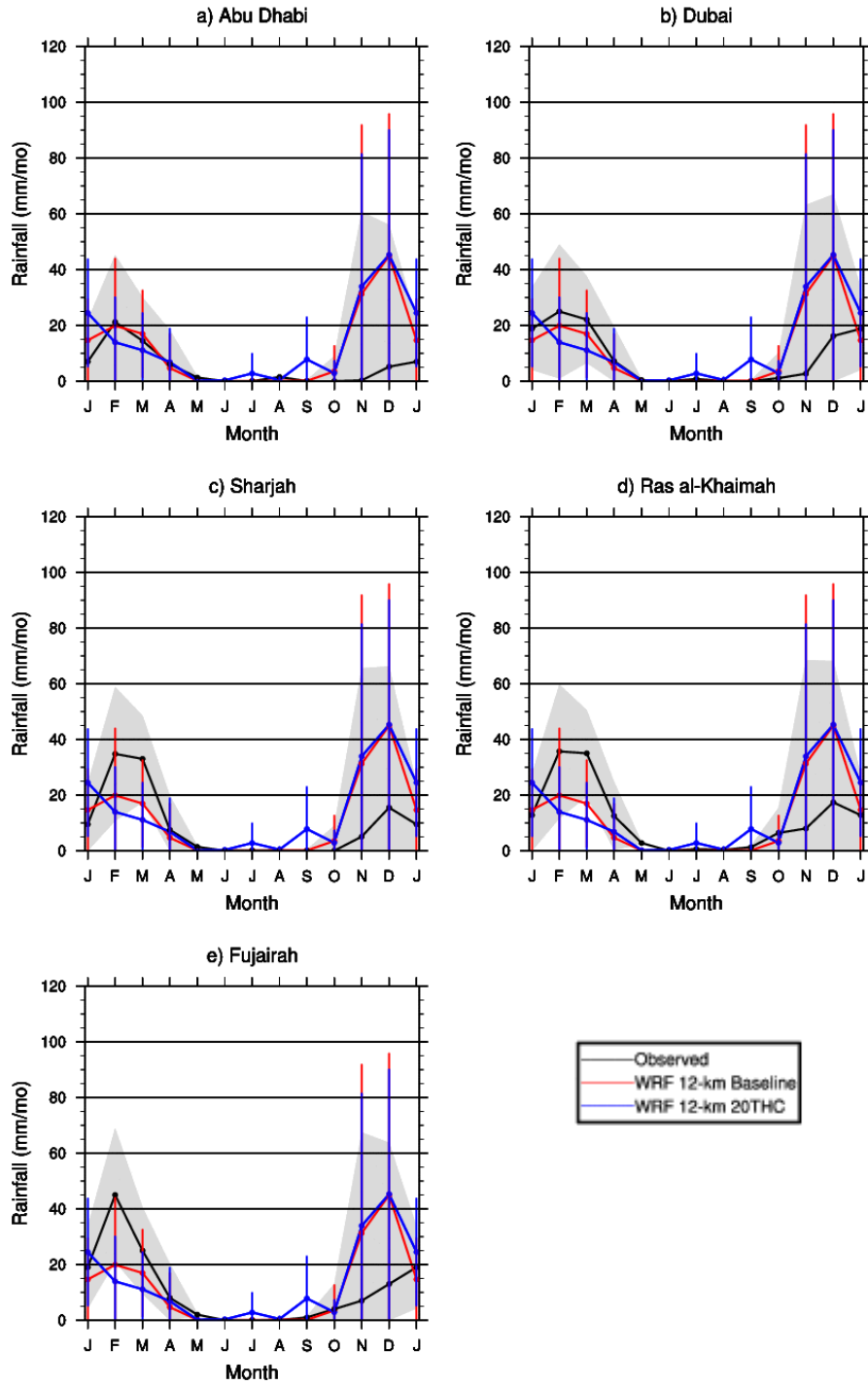
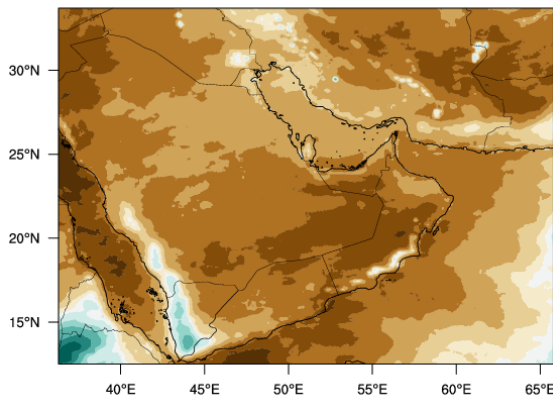
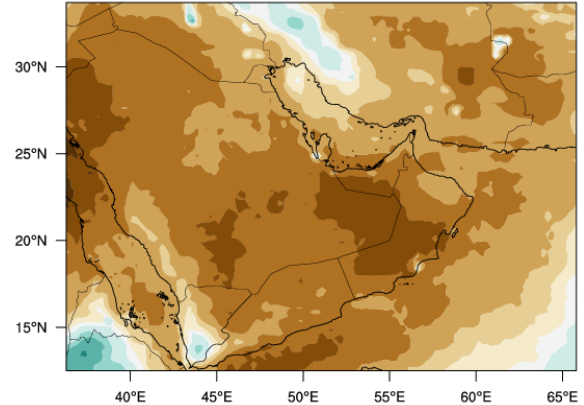
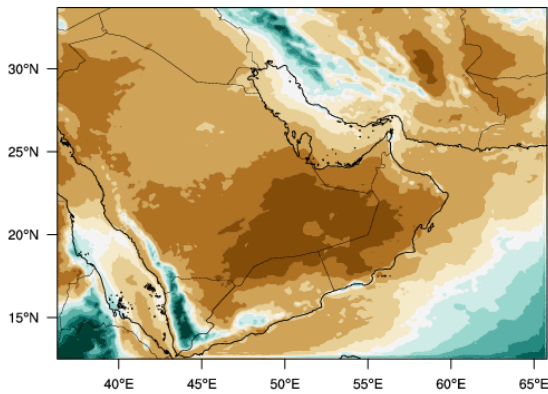
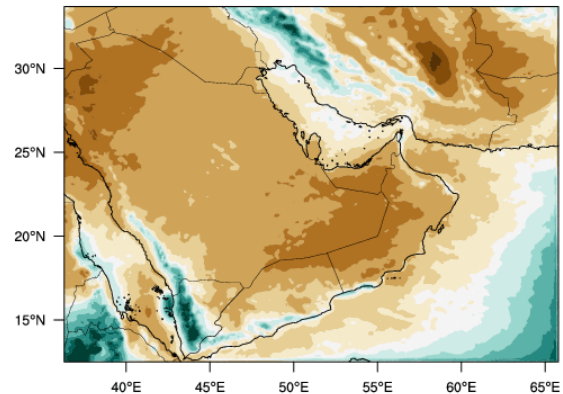


Figure 15. Same as Figure 14, but for precipitation.



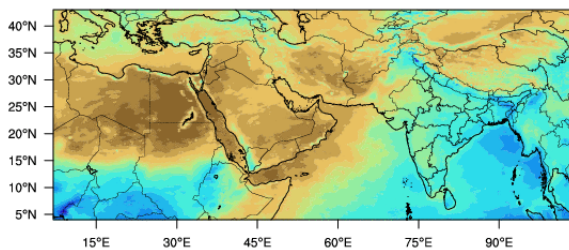
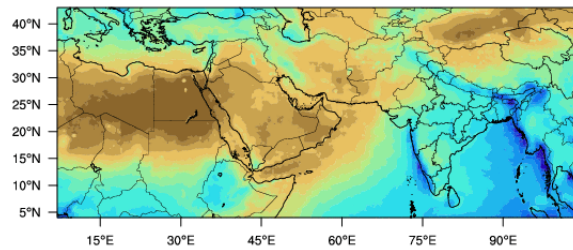
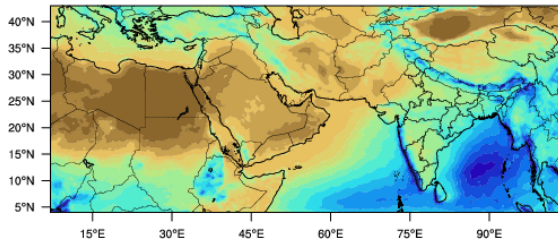
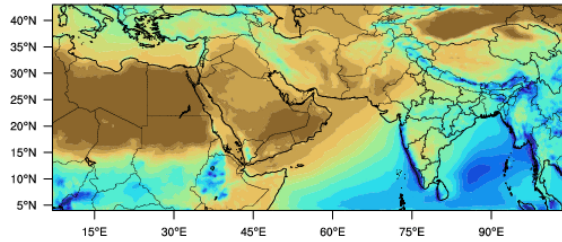
Figure 16 shows the annual average precipitation for the entire 12-km region (D2), with the top panel are satellite derived estimates of TRMM and CMORPH and the bottom panel the Baseline (WRF driven by ERA-Interim) and 20THC (WRF driven by bias-corrected CCSM4). Note that there are differences among the satellite estimated rainfall, with CMORPH showing greater amounts over the western Iranian border when compared with TRMM. The 12-km WRF simulated precipitation shows the model's fidelity to capture complex patterns of precipitation, including the higher amounts in western Iran, the smaller amounts over the southeastern and the higher amounts on the southwestern Arabian Peninsula,

**TRMM**

**CMORPH**

**WRF 12-km Baseline**

**WRF 12-km 20THC**


**Figure 16. Annual precipitation estimates for the entire 12-km domain and from a) NASA's TRMM sensor (~25 km resolution; 1999-2011 average), b) the CPC CMORPH product (~8 km resolution; 2003-2009 average), c) the WRF "Baseline" simulations driven by ERA-Interim (12-km resolution, 1986-2005 average), and d) the WRF 20THC simulations driven by CESM (12-km resolution, 1986-2005 average).**

Figure 17 shows the current day simulation of precipitation over the largest domain (D1), which is the 36-KM domain. The figure includes the TRMM and CMORPH precipitation

climatologies (top) and the WRF simulations forced by ERA-Interim (WRF 36KM Baseline) and forced by the bias-corrected CCSM4 model over the contemporary period. The patterns of rainfall are similar when the observations are compared with the simulations, with the WRF Baseline run generally showing greater amounts of rainfall off the eastern Indian coast. Even at 36-km resolution, the WRF model is able to simulate the strong precipitation gradient at the southwestern corner of the Arabian Peninsula and the Red Sea, the higher precipitation amounts over the Ethiopian Highlands of eastern Africa, and the Arabian Gulf-Western Iran precipitation boundary. So while there is a somewhat wet bias in the simulation, the spatial patterns of precipitation appear to be adequately represented across this large domain.

**TRMM**

**CMORPH**

**WRF 36-km Baseline**

**WRF 36-km 20THC**


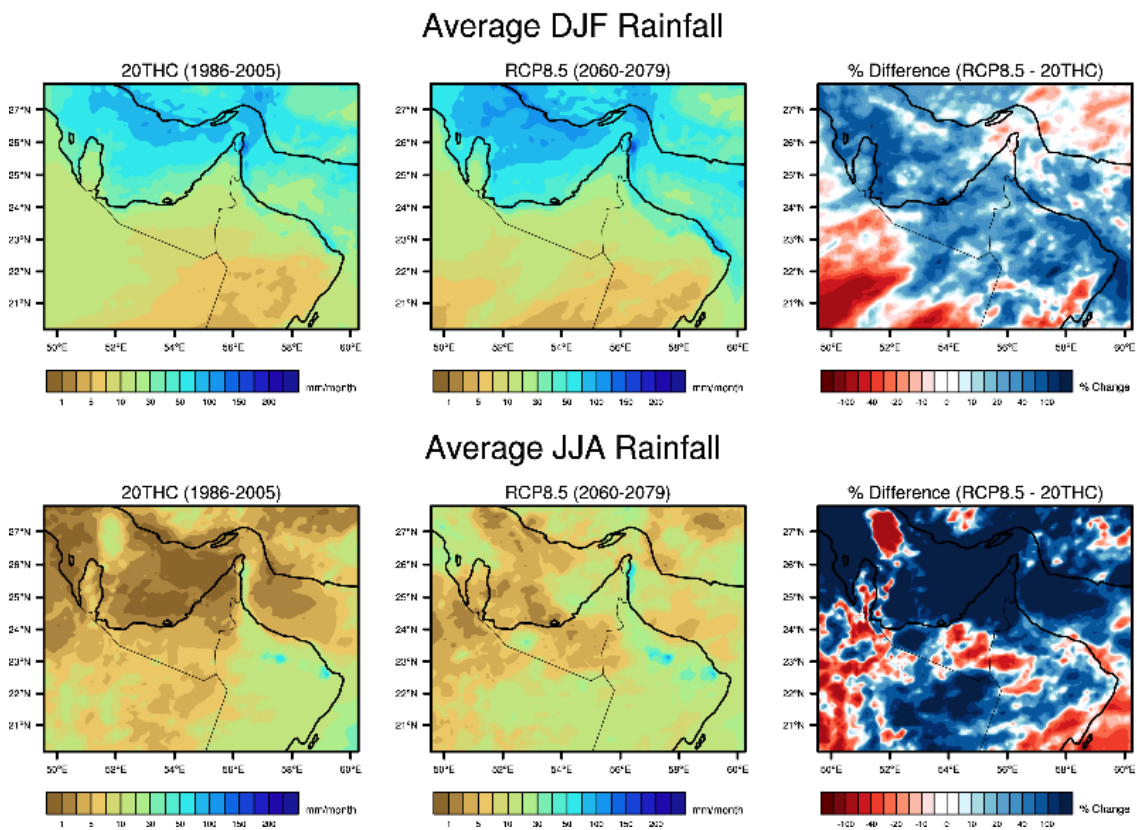
**Figure 17.** Annual precipitation estimates for the entire 36-km domain and from a) NASA's TRMM sensor (~25 km resolution; 1999-2011 average), b) the CPC CMORPH product (~8 km resolution; 2003-2009 average), c) the WRF "Baseline" simulations driven by ERA-Interim (12-km resolution, 1986-2005 average), and d) the WRF 20THC simulations driven by CESM (12-km resolution, 1986-2005 average).

### 3.4 Projections of future climatic change with CCSM4

To estimate the projected precipitation changes over the UAE and Arabian Peninsula, WRF simulations were run (using the bias-corrected CCSM4 forcing) for three time periods: present-day conditions (1986-2005, denoted as "20THC"), and for the RCP 4.5 and RCP 8.5 scenarios (2060-2079, denoted as "RCP4.5" and "RCP8.5"). Additional focus is given to the RCP8.5 scenario as compared to RCP4.5, because RCP8.5 is the more aggressive greenhouse gas emissions trajectory that is most similar to humankind's current trajectory.

**Precipitation-** Figure 18 shows the projected rainfall amounts for 20THC (left column), RCP8.5 (center column), and the percentage difference (right column), averaged annually (top row),

winter (December-January-February, middle row), and summer (June-July-August, bottom row). In total (top row), rainfall is projected to increase over much of the UAE, the Hajar Mountains, and Qatar. Increases of 50-100% from current amounts are projected for portions of Dubai, Sharjah, and the northern Abu Dhabi emirates, with increases averaging around 25% over surrounding regions. Increases are also projected over the Arabian Gulf and Gulf of Oman. Decreasing rainfall is projected over much of Oman and eastern Saudi Arabia. Winter (DJF) is the dominant season for rainfall across the region (middle row), and the projected rainfall increases over the Arabian Gulf and north of the Hajar Mountains primarily occur during this season. Interestingly, during the dry summer season, rainfall increases over much of the UAE are larger than during the wetter winter season, in both absolute value and percentage change. The rainfall increases over the Hajar Mountains and the eastern UAE primarily occur during summer as well. The annual decreases over much of Oman and eastern Saudi Arabia occur during winter and spring (March-April-May, not shown).



**Figure 18.** WRF precipitation estimates for the 20THC simulation (left column), RCP 8.5 simulation (center column), and the difference (percentage change of RCP 8.5 minus 20THC; right column). Top row is averaged for winter (December, January, and February) bottom row is averaged for summer (June, July and August).

The annual cycle of precipitation for the WRF 20THC simulations (1986-2005) is compared with the WRF RCP4.5 (Figure 19) and RCP8.5 (Figure 20) simulations for 2060-2079 for five cities in UAE. While both future projections indicate an overall increase in precipitation,

consistent with the spatial plots shown in Figure 18, the RCP4.5 simulations exhibit a larger winter precipitation increase despite having lower greenhouse gas forcing. The RCP8.5 simulations, by contrast, exhibit larger summer and early autumn (convective) precipitation increases. However, all results should be interpreted with caution: the future precipitation changes are statistically insignificant or only weakly statistically significant during some winter months ( $p < 0.10$ ), suggesting a great deal of noise in the signal. Inspection of the uncertainty bars in Figure 19 and Figure 20 suggests that, in general, the variability of precipitation may increase in the future, especially for the RCP8.5 scenario.

Despite the projected increases in rainfall over much of the UAE, the number of wet days is actually projected to *decrease* in the RCP8.5 future climate scenario over the UAE. Figure 21 shows the Wet Days Index for the WRF 20THC and RCP8.5 simulations, and the differences. The Wet Days Index is simply the number of days (per year, averaged over the respective 20-year periods) with rainfall greater than 1 mm. With precipitation increases projected to occur over relatively wet portions of the plotted region, the projected decrease in the Wet Days Index, strong precipitation increases during summer, and the projected temperature increases (see next section), a thermodynamic explanation for the rainfall increases is suggested. This simply involves the increase in saturation vapor pressure with increasing temperature (the Clausius-Clapeyron equation). The Clausius-Clapeyron equation predicts the temperature dependence of vapor pressures of liquids and/or solids. Larger amounts of rainfall would occur during comparatively fewer rainfall events than currently observed. This explanation is consistent with an increase in the variability (i.e., volatility) of precipitation.



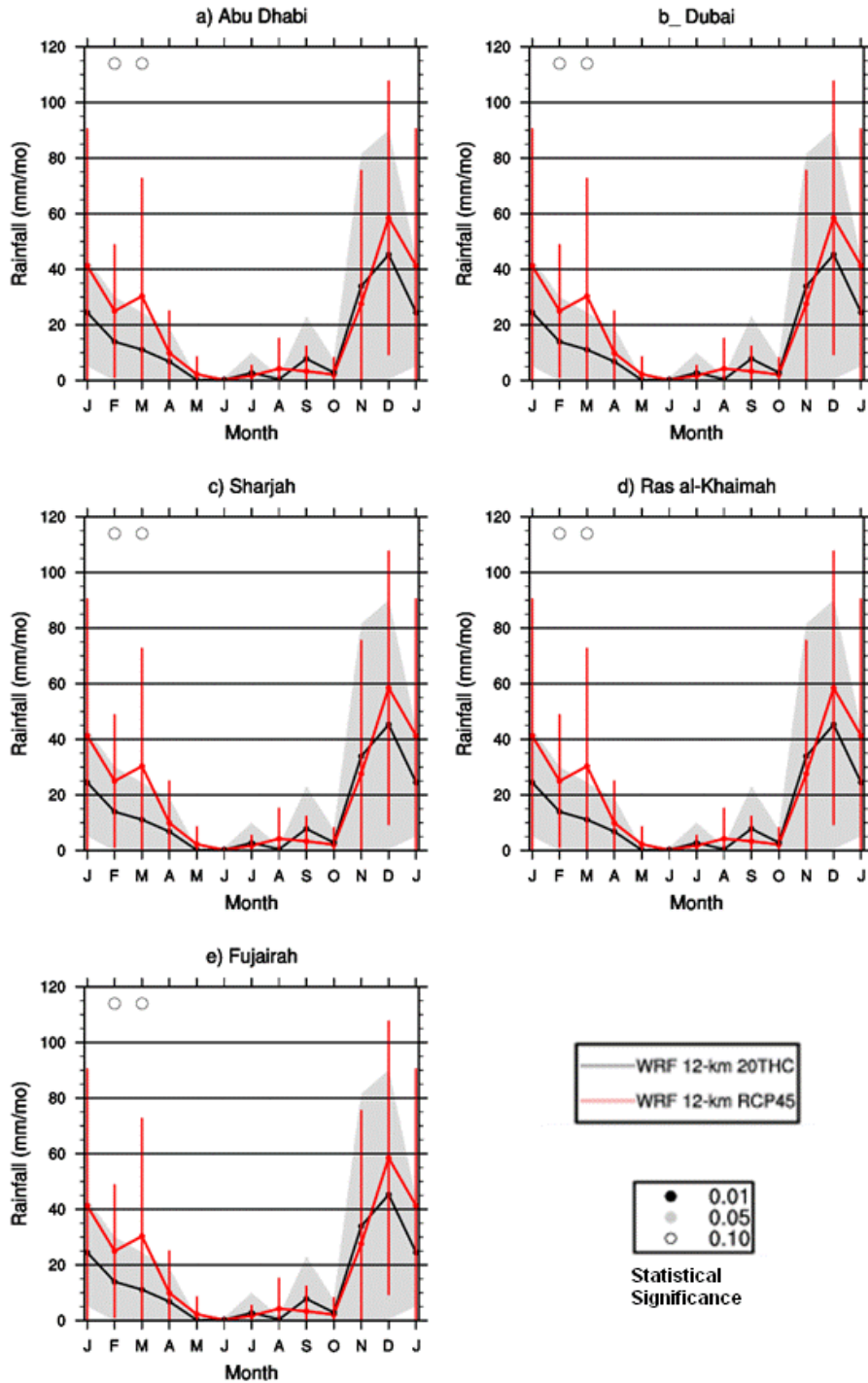


Figure 19. Annual average monthly precipitation for 20THC (1986-2005) versus future RCP4.5 (2060-2079) simulations in five UAE cities. Future changes in precipitation that are statistically significant are indicated by dots near the top of each graph, the color of which indicates the level of significance (see legend). Error bars indicate standard deviations of monthly means.



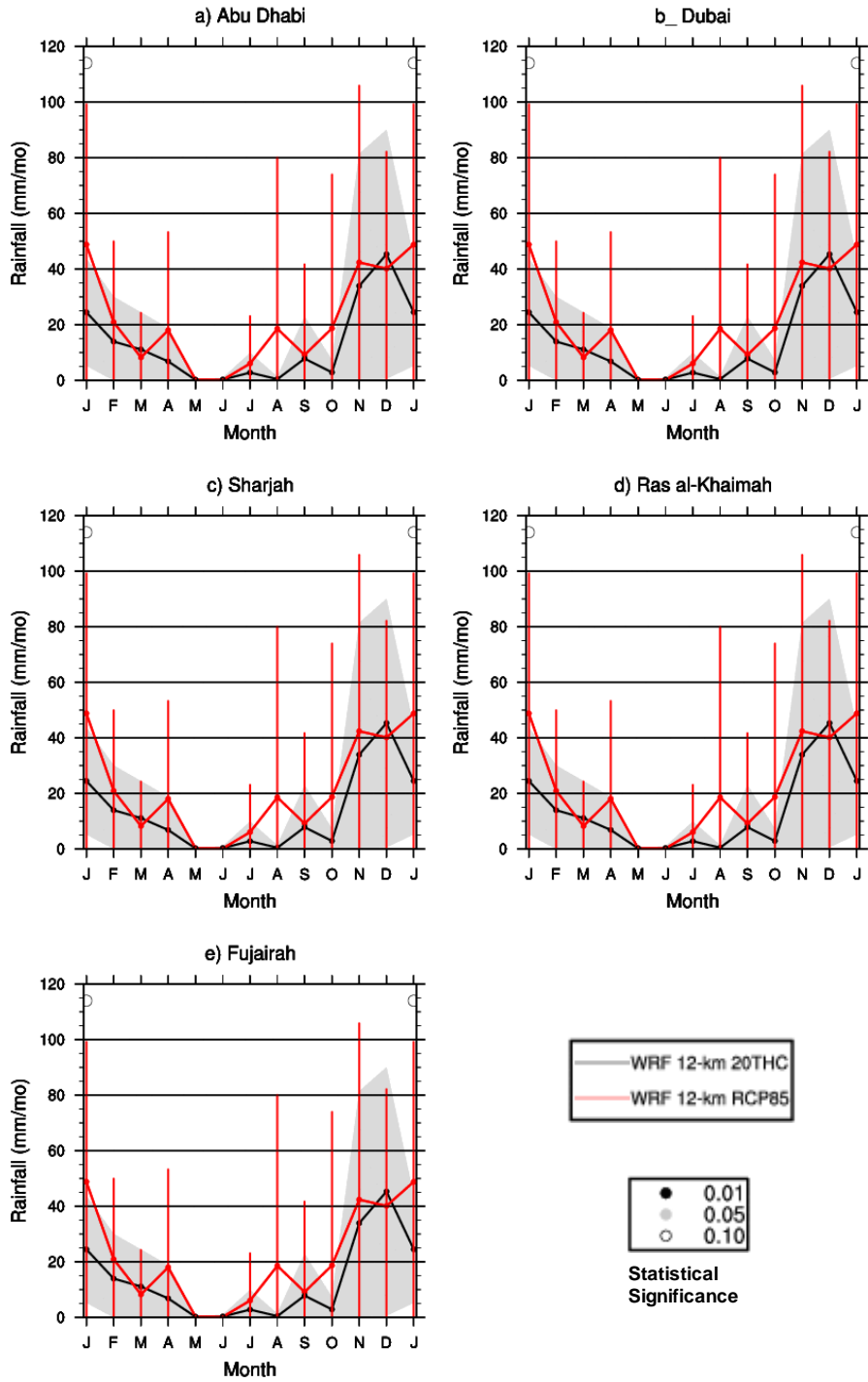


Figure 20. Same as Figure 19, but for the RCP8.5 scenario.

## Wet Days Index

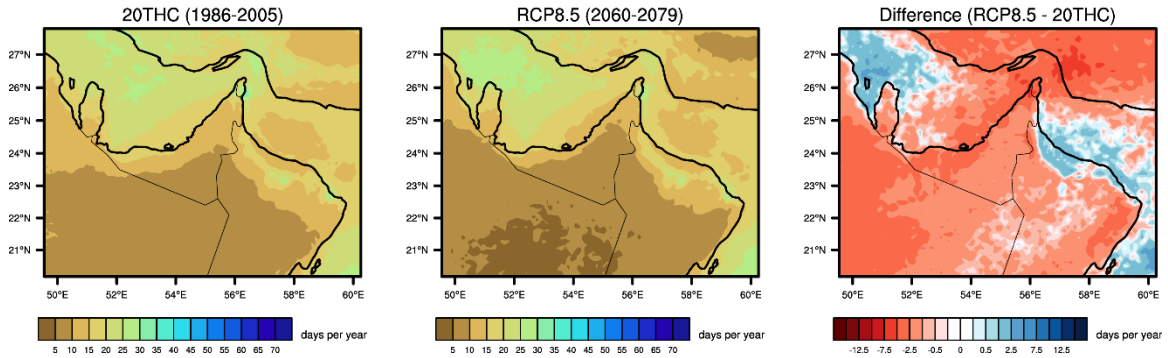
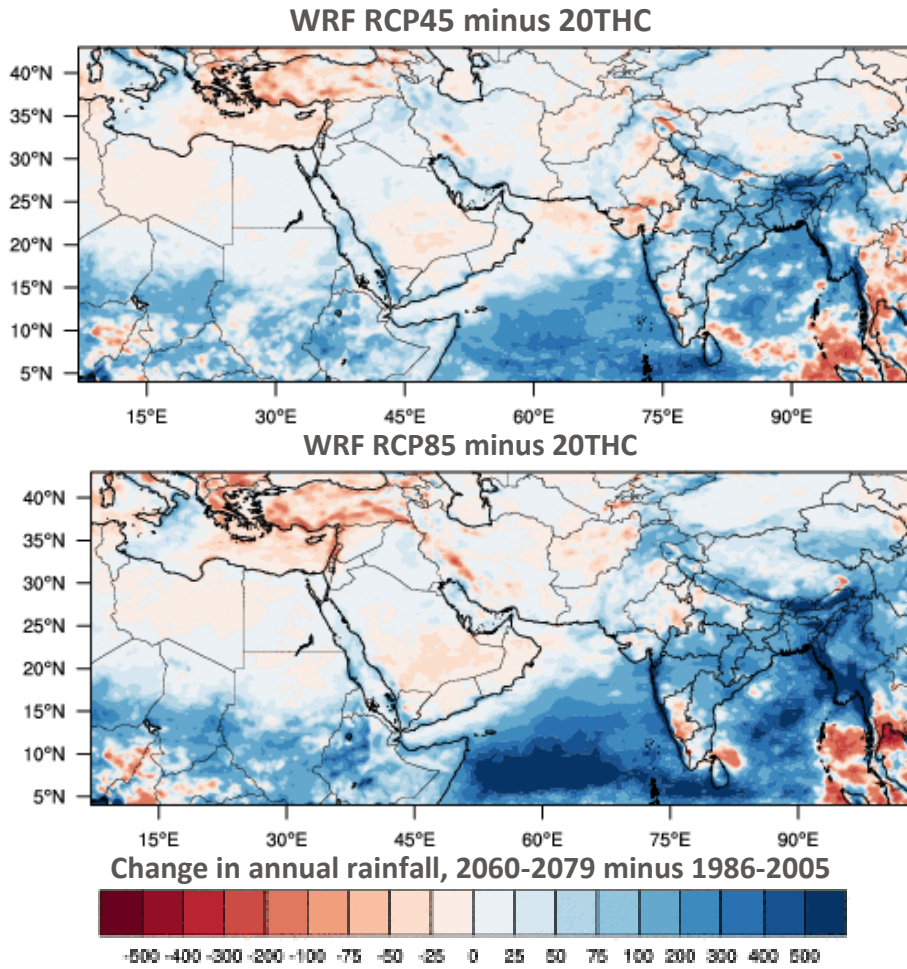


Figure 21. Wet Days Index values (the number of days with rainfall greater than 1 mm, summed over the 20-year time periods), for 20THC (left), RCP 8.5 (center), and the difference (RCP 8.5 minus 20THC; right).

Figure 22 shows the regional change in precipitation for the RCP45 and the RCP85 relative to the 20THC climate for the 36-km domain. One can identify a complex pattern of changing rainfall, with a drying over central northern Africa and southern Arabia and wetter oceans.



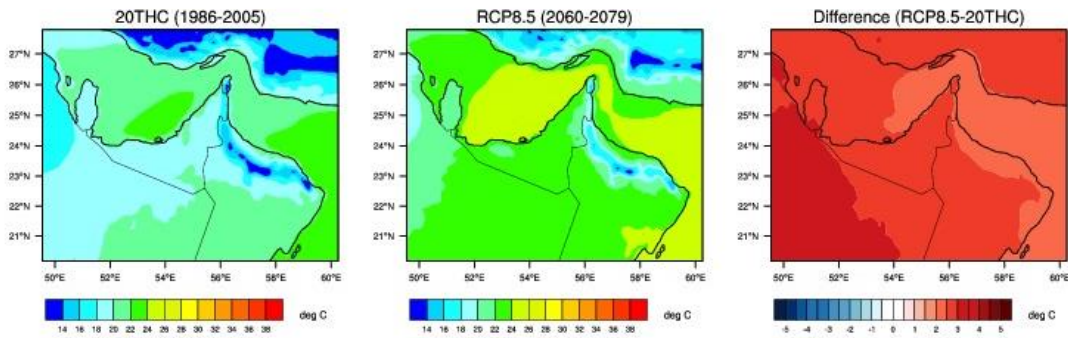
**Figure 22. Projected change in precipitation over the 36-km domain for the RCP4.5 and RCP8.5**

**Temperature and Humidity**

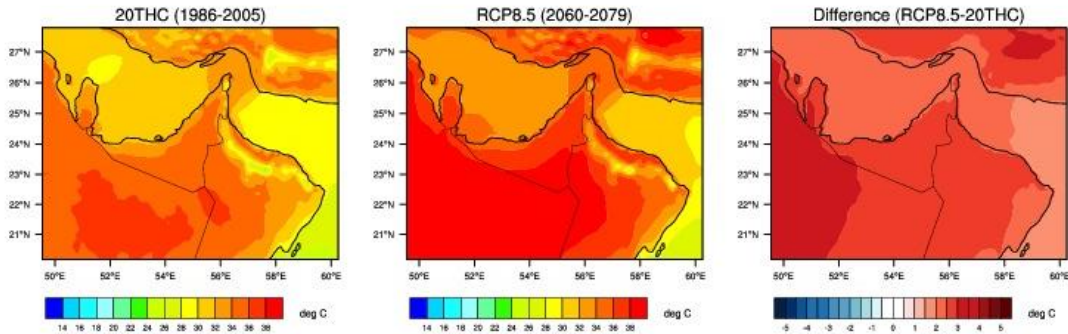
The projected daily average 2-m air temperature and 10-m specific humidity changes are shown in Figure 23 and Figure 24 for the winter (December, January, and February) and summer (June, July, and August) periods, respectively. Average future temperature increases are unanimous across the plotted domain, on the order of 2°-3°C over land areas. Increases are slightly smaller over many coastal areas. These changes are consistent across winter and summer.

Humidity changes are greater in the summer months, associated with the greater water holding capacity of the warmer atmosphere and are about 10% greater over the Arabian Gulf, with higher humidity across most of the UAE and proportionally more in the northeastern corner of the country associated with greater humidity over the Arabian Sea.

**Average DJF Temperature**

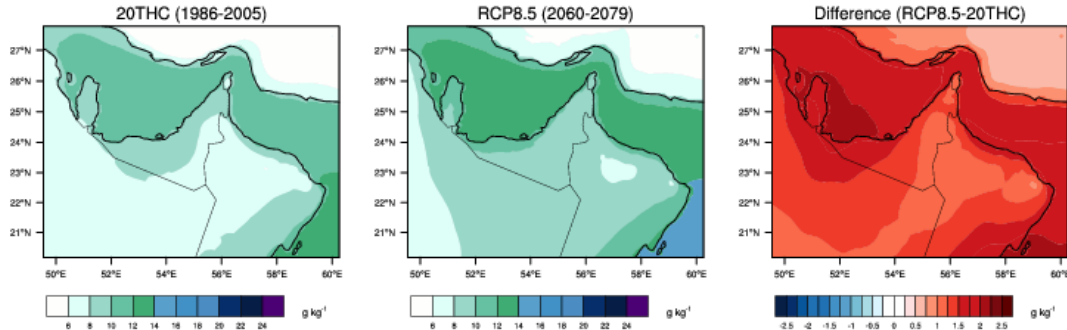


**Average JJA Temperature**



**Figure 23. Average DJF (top) and JJA (bottom) 2-m Air Temperature (°C), for 20THC (left), RCP 8.5 (center), and the difference (RCP 8.5 minus 20THC; right).**

### Average DJF Specific Humidity



### Average JJA Specific Humidity

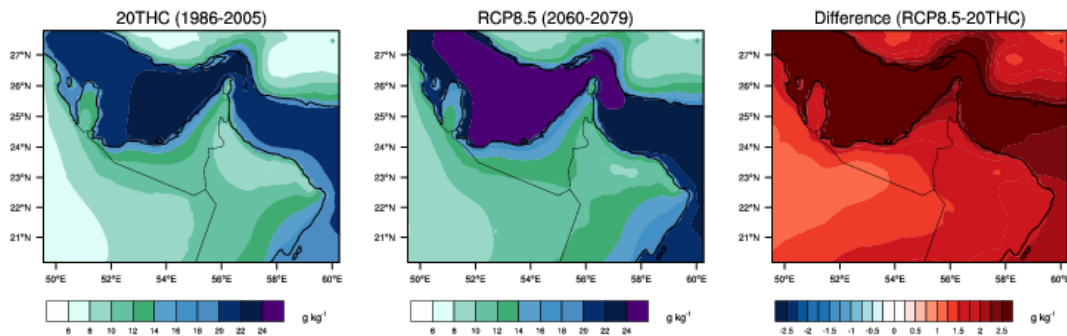


Figure 24. Average DJF (top) and JJA (bottom) 2-m Specific Humidity (g/kg), for 20THC (left), RCP 8.5 (center), and the difference (RCP 8.5 minus 20THC; right).

The annual cycle of 2-m air temperature for the WRF 20THC simulations (1986-2005) is compared with the WRF RCP4.5 (Figure 25) and RCP8.5 (Figure 26) simulations for 2060-2079 for five cities in UAE. Temperatures are projected to statistically significantly increase ( $p < 0.01$ ) in all months and for both the RCP4.5 and RCP8.5 scenarios, for all five cities. The magnitude of the projected temperature increases is remarkably consistent across months and cities, being on the order of  $+2^{\circ}\text{C}$  for the RCP4.5 scenario, and  $+3^{\circ}\text{C}$  for the RCP8.5 scenario. The greatest amount of warming is over the interior of Saudi Arabia, where the warming is on the order of  $+4^{\circ}\text{C}$  within the interior of the region.

## RCP4.5

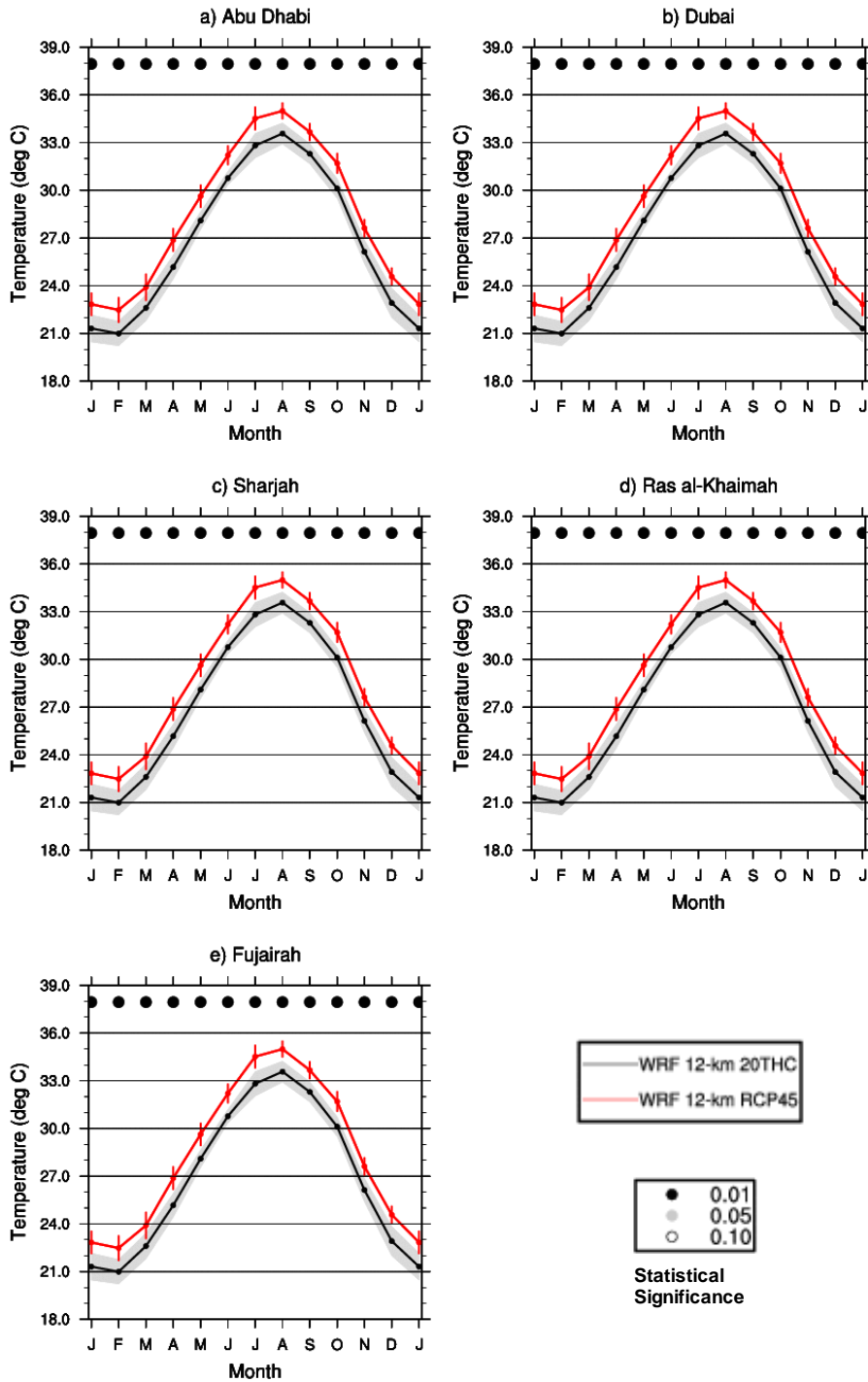


Figure 25. Monthly average temperature for 20THC (1986-2005) versus future RCP4.5 (2060-2079) simulations in five UAE cities. Future changes in temperature that are statistically significant are indicated by dots near the top of each graph, the color of which indicates the level of significance (see legend). Error bars and shading indicate standard deviations of monthly means.



## RCP8.5

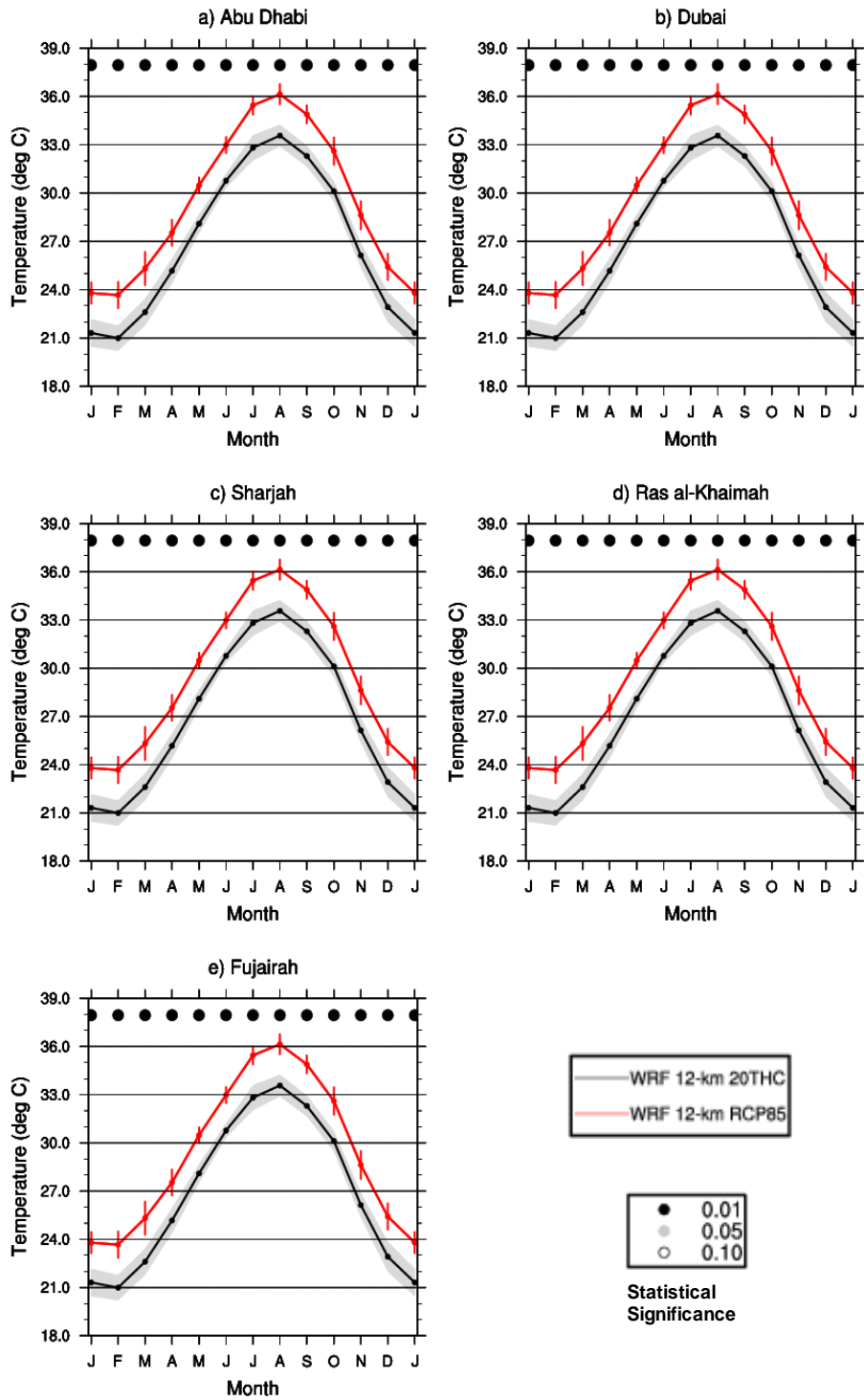


Figure 26. Same as Figure 25, but for the RCP8.5 scenario.

Future projected changes in temperature are expressed as the *Heat Wave Duration Index* (HWDI) in Figure 27. This metric is defined as the number of days, in intervals of 6 days, that the daily maximum temperature is greater than 5°C above a reference value. In this case, the reference value is the respective 20-year average of the daily maximum temperature for each calendar day. HWDI values are small for 20THC, likely reflecting the relatively small year-to-year variance in temperature across the region, as the day-to-day variance in temperature in region is relatively low (e.g. in the summer, it is nearly always very warm). When HWDI is calculated for the RCP8.5 future climate scenario, using the corresponding RCP8.5 averages as reference, there is a marked decrease in HWDI across most of the UAE, the Hajar Mountains, and portions of eastern Saudi Arabia. Increases in HWDI are restricted to a few coastal areas around the plotted domain. The decrease in HWDI may be explained by the projected increase in average temperature (Fig. 3.11) restricting the number of *relatively* hot days in the future climate scenario.

### Heat Wave Duration Index

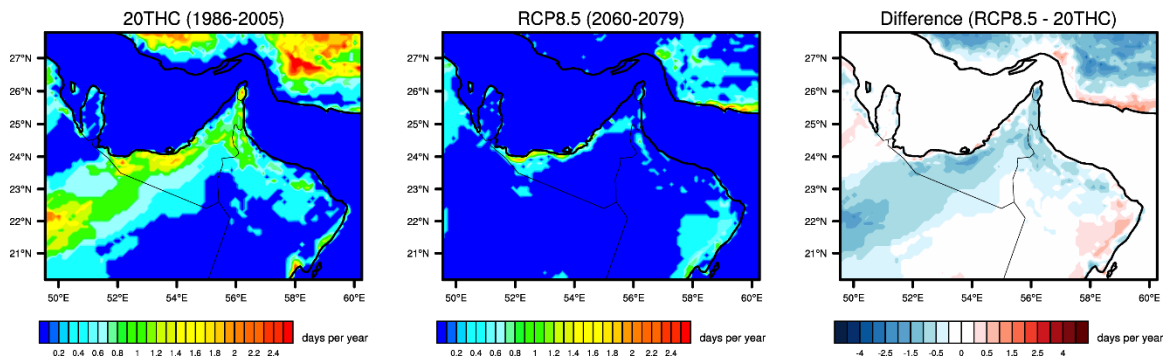


Figure 27. Heat Wave Duration Index values (the number of days, in intervals of 6 days, that the daily maximum temperature is greater than 5°C above a reference value), for 20THC (left), RCP 8.5 (center), and the difference (RCP 8.5 minus 20THC; right).

### 3.5 Changes in Wind around Abu Dhabi Island

Figure 28 shows the December-January-February (DJF) mean morning (0600 local) and early evening (1800 local) 10-meter winds for the current 20<sup>th</sup> century climate (20THC) and the future climate for the RCP8.5 CCSM projection from the 4-km, 10-year simulations. The far-right panel shows their difference. Note that in the early morning, DJF, the wind is from the northeast off of the Arabian Gulf Coast, and under the current climate conditions (20<sup>th</sup> THC), the wind from the interior of the UAE is weaker than in the future climate; resulting in a net change in early morning wind from the east to the west or outward into the Arabian Gulf. This is likely the result of a weakening of the ocean-land temperature gradient, which normally gives rise to an onshore sea breeze, particularly in the afternoon hours. There is a relatively persistent warmer, interior environment relative to Arabian Gulf Waters (see Figure 10 and Figure 23) that results in a more northwesterly near surface wind and a weakening of the sea-breeze. Note that evening wind fields (1800) are still similarly strong under the

current and future climate, with a generally southwesterly change in flow, with a change of about 0.5 m/s over Abu Dhabi Island, which is about a 20% change in the mean wind velocity.

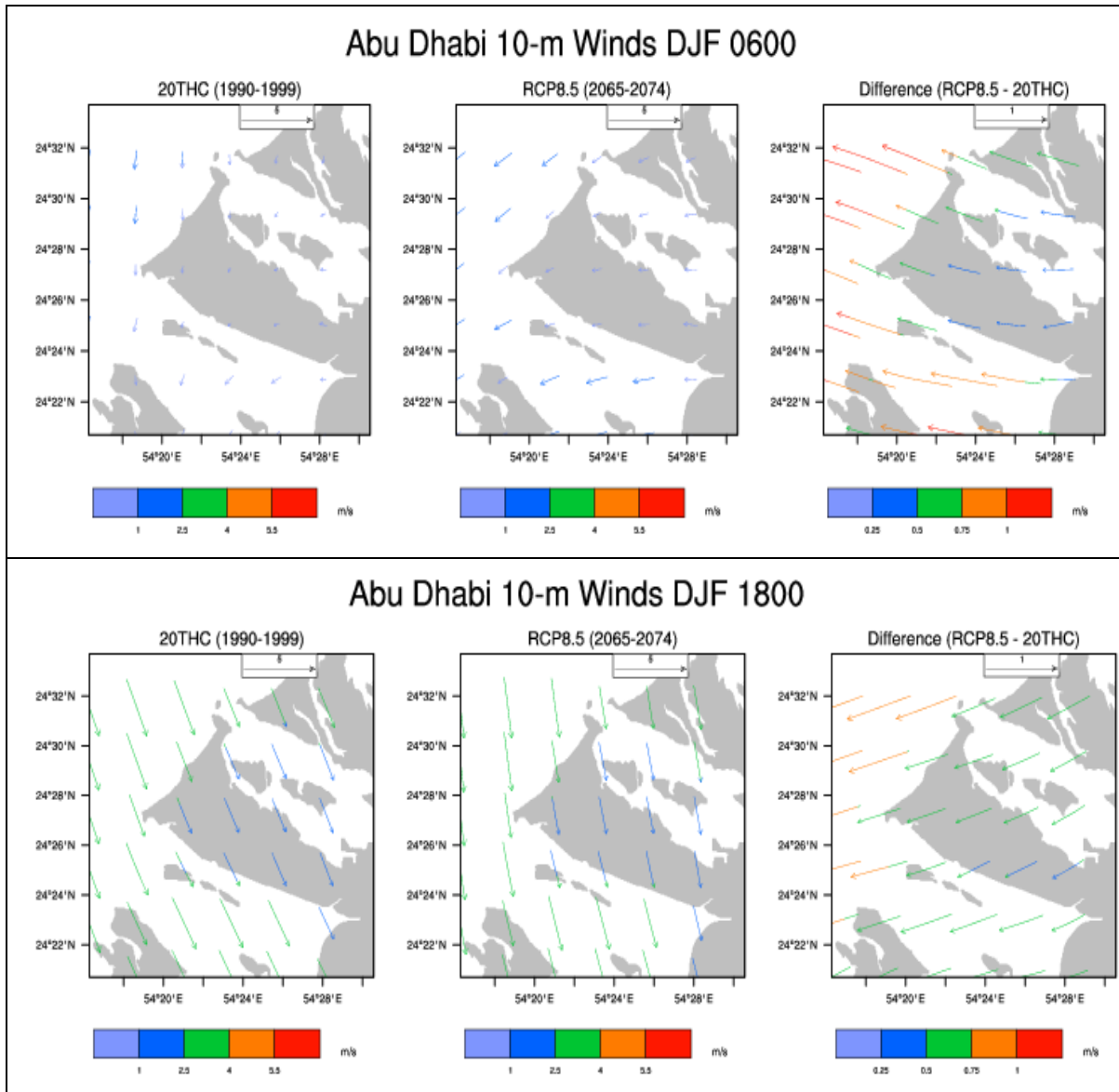


Figure 28. Mean 10-m winds around Abu Dhabi Island for DJF, early morning local time (0600) (top) and the early evening local time (1800) (bottom).

Figure 29 is the same Figure 28, except that the mean wind field is estimated for the months of June, July and August (JJA). Figure 29 (top) is the mean morning hour (0600), 10-m wind, while Figure 29 (bottom) is for the evening hour (1800). Summertime, morning hour winds are weak in both the current and future climate simulations, with a net change of flow to the north-east. A relatively strong, on-shore sea-breeze develops in the evening hour, with a net change in wind similar to the morning hour, with a slight in magnitude to the northeast.

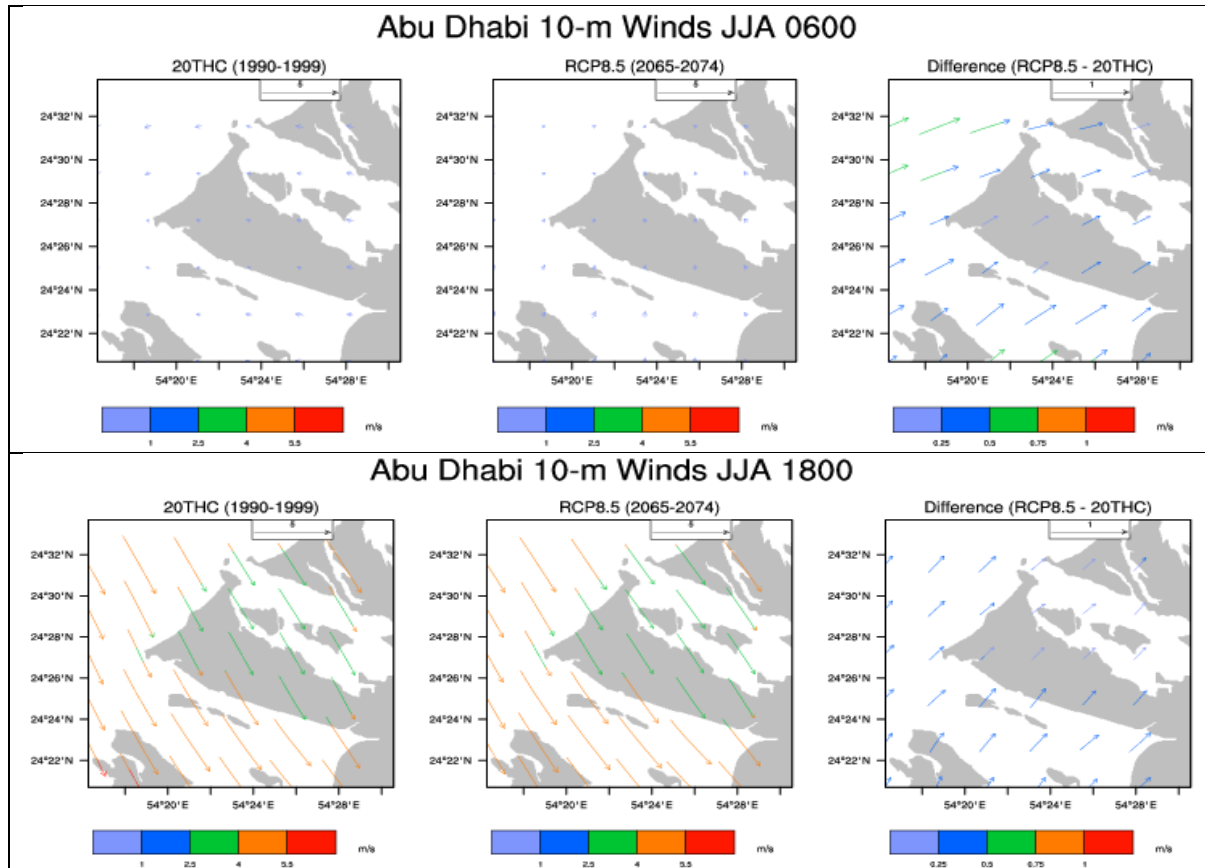


Figure 29. Mean 10-m winds around Abu Dhabi Island for JJA, early morning local time (0600) (top) and the early evening local time (1800) (bottom).

### 3.6 A Climate Anomaly in the CCSM4 Forcing and its implication for the WRF Results

Since the WRF regional climate model is driven by the boundary forcing from the CCSM4 global climate model, it significantly reflects the conditions of the driving model. During the course of our analysis of the WRF results at both the 12-km and 4-km resolutions, we noticed some interesting meteorological events imbedded within the regional climate model simulations. Most notably, were some intense cyclones that originated in the Arabian Sea, off the west coast of India, which propagated westward towards the Arabian Peninsula and the UAE. Figure 30 shows one such event that occurs in CCSM4 in September of 2066, where the colored grid is sea-level pressure, and the black lines show only the 950 to 995 hPa contours, which are indicative of a tropical typhoon. Note that this event remains coherent through a 6-day period, reduces in intensity when it makes landfall and strikes the Oman/UAE coast, and then re-intensifies as it tracks into the Arabian Peninsula. This is quite a remarkable event. First, that the CCSM4 generates such a tropical cyclone and then that the event persists so long across the region including across the Arabian Peninsula.



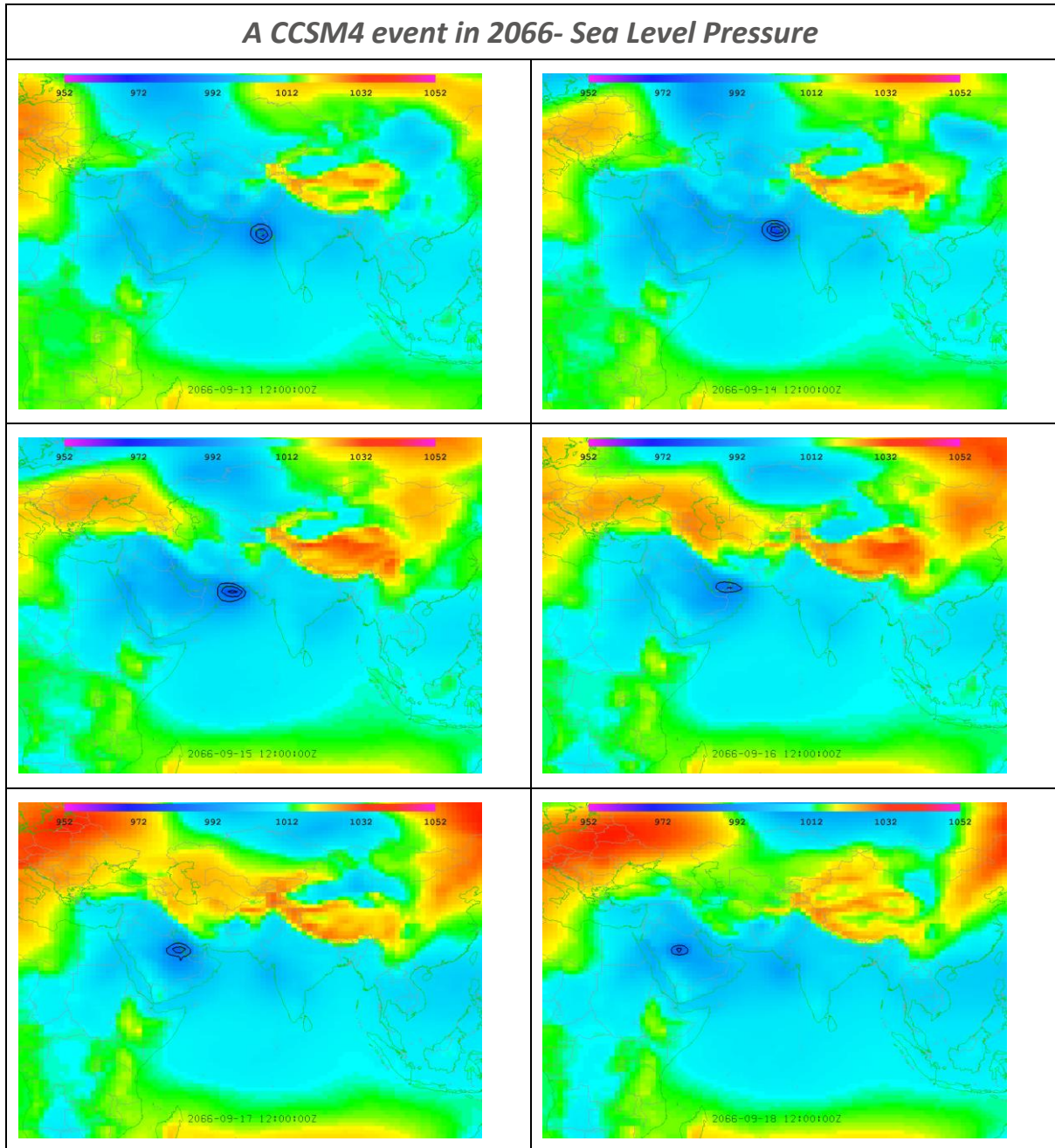


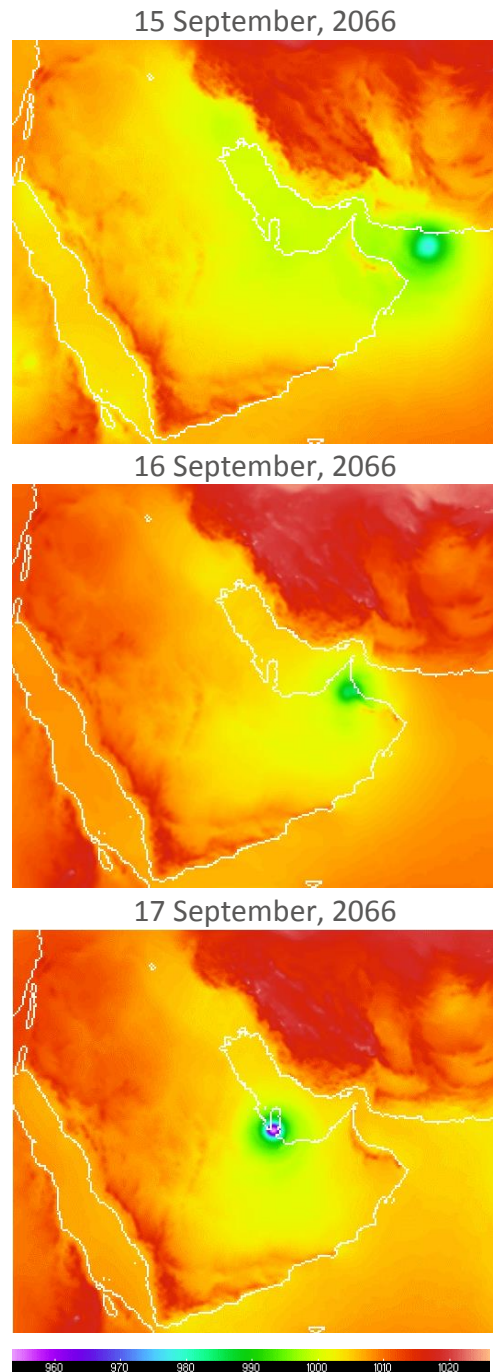
Figure 30. A future cyclone in the CCSM4 model that tracks first across the Arabian Sea and then the Arabian Peninsula, showing sea-level pressure for the color-composite grid and a minimum contour range of 950 to 995 (hPa) in black. The top-left image is for 13 September, the top-right image is for 14 September, etc. The bottom-right panel is for 18 September, when the event is over the Arabian Peninsula.



Figure 31 shows sea level pressure, rendered over this same event for three daily time slices at 0Z on Sept 15, 16, and 17, as simulated by WRF model from the D2 or 12-km domain. While the year is marked as 2066, it is important to realize that this is not a forecast or prediction of an event of this nature occurring at this particular time in the future. Rather, the CCSM4 GCM has spawned a large cyclonic event during this period (Figure 30), and if a different ensemble member from the CCSM4 runs were selected or the model was re-run with a new set of initial conditions, it is highly unlikely that this event would occur again at this particular time and with the intensity and storm track that it took. However, it is likely that other ensemble members from the IPCC AR5 archive of CCSM4 output contain cyclonic events in the region that includes the Arabian Sea and the surrounding region.

As we noted in the analysis of the CCSM4 output shown in Figure 30, this storm event maintains itself across the Arabian Peninsula. This is most likely due to the fact that the CCSM4 is relatively coarse, as the known terrain barrier of the Oman Mountains is not adequately reflected in the model and therefore there is little to impede the western movement of the storm. Note, too, that CCSM4 GCM tends to increase the relative area of the open ocean relative to the land area around the Gulf of Oman (see Figure 4). This likely another factor in the persistence and intensification of the cyclone in the region.

This event suggests a cautionary note on the use of dynamical models like WRF, when drawing broad conclusions about regional change. This event was identified while analyzing the change from the current and future 20-year simulations. We noted some large increases in precipitation, over the region in the future climate simulation, which were largely due to precipitation increases from a few events, such as the cyclone



**Figure 31. Sea-Level pressure (hPa) as simulated by the 12-km, D-02 domain.**

summarized in this report. Therefore, drawing conclusions about mean changes, particularly for precipitation should be made cautiously.

## 4. Summary

This Regional Atmospheric Modeling sub-project demonstrated the development of a novel, bias-corrected global climate model dataset, based on NCAR's Community Climate Systems Model (CCSM4). The CCSM4 was one the IPCC AR5 global climate models, which was bias-corrected to be statistically similar to the European Centre for Medium-Range Weather Forecasting (ECMWF) Interim Reanalysis (ERA-Interim; Dee et al. 2011) dataset. The ERA-Interim is considered to be the most accurate atmospheric reanalysis available at the present time (e.g., Lorenz and Kunstmann 2010). The bias-corrected, CCSM4 dataset was then used as the boundary and initial conditions, to force the NCAR Weather Research Forecast (WRF) to dynamically downscale the climate of the 20<sup>th</sup> century and the future climate based on the RCP8.5 emission pathway. The WRF model was run at spatial resolutions of 36, 12, and 4-km that included a large portion of the Arabian Peninsula. The 12 and 36 KM domains were run for a longer period, 2006 to 2100, while the 4-km domain (D3) was run for two shorter, 10-year periods. Nearly one million "core-hours" on the NCAR supercomputer were used for these analysis. A core-hour is essentially the number of processor cores used multiplied by the duration of the job, so had a single quad-core personal computer been used, the runs would have taken more than 30-years to complete.

The results show that the WRF simulations adequately captured the regional climate of the Arabian Peninsula for the 20<sup>th</sup> century period. The CCSM4 projection of the future climate indicates generally wetter and warmer conditions in the region, with the CCSM4 projected trends similar to the ensemble average of all the GCMs used in the IPCC AR5 experiments (e.g. warm and wet). This means that the use of the CCSM4 as a single GCM boundary forcing for the regional WRF model is likely representative of a larger ensemble of climate models.

Most of the increased rainfall is associated with wetter conditions over the Arabian Peninsula that extends across a large portion of the UAE. We discovered some interesting attributes that are embedded within the CCSM4 climate projection (i.e. the *r6i1p1* experiment from the CCSM4 ensemble member run), most notably some large tropical cyclones that propagate across the Arabian Peninsula. Heavy precipitation is associated with these storms, and likely skews the representation of "average" precipitation change, especially in the arid and hyper-arid regions of the Arabian Peninsula. We demonstrated some tailored climate indices that can be developed from the WRF dataset (Wet and Dry indices and Heat Wave Duration Index), and demonstrated possible changes in wind fields around and near Abu Dhabi Island. Other indices can be derived from the dataset upon request and the dataset is being provide to the EAD on a hard-drive and will be made accessible via a web portal in the spring of 2015.

## 5. Future Research

The results point to several promising areas of future research. Building off the datasets generated by the study, these include:

- *Addressing uncertainty.* Additional WRF runs using multiple Coupled Atmosphere Ocean Global Circulation Models to generate a large ensemble of future projections
- *Projecting tropical storm frequency.* Additional WRF runs using its "simple ocean" representation to simulate tropical storms, including surface flux/drag formulations for high-winds an approach to capture impacts of sea surface temperatures on cyclones.
- *Coupling atmosphere and oceans.* Running experiments in a coupled fashion would allow a fuller understand of how atmospheric and Gulf dynamics work together. As the ocean modeling found, circulation and salinity are quite sensitive to the state of the atmosphere.
- *Projecting weather extremes.* There are some extraordinary cyclonic events in the CCSM4 GCM data out towards the end of the 21st Century. Exploring if other GCMs produce these kinds of events would be valuable.
- *Optimizing modeling configurations.* Because the WRF model has multiple configurations, it would be beneficial to conduct more experiments to ensure that an optimal configuration has been achieved for a multitude of meteorological events.
- *Sandstorm/dust modeling.* Given the importance of dust, it would be valuable to explore how changing climate might impact dust formation, transport and deposition in the region.

## 6. References

- Bruyère CL, Done JM, Holland GJ, Fredrick S. 2013. Bias corrections of global models for regional climate simulations of high-impact weather. *Clim. Dyn.*, doi:10.1007/s00382-013-2011-6.
- Dee DP, and Coauthors, 2011. The ERA-Interim reanalysis: configuration and performance of the data assimilation system. *Q. J. R. Meteorol. Soc.* **137**: 553-597.
- Done JM, Holland GJ, Bruyère CL, Leung LR, Suzuki-Parker A. 2013. Modeling high-impact weather and climate: lessons from a tropical cyclone perspective. *Climatic Change*, doi:10.1007/s10584-013-0954-6.
- Gent PR, Danabasoglu G, Donner LJ, Holland MM, Hunke EC, Jayne SR, Lawrence DM, Neale RB, Rasch PJ, Vertenstein M, Worley PH, Yang Z-L, Zhang M. 2011. The Community Climate System Model version 4. *J. Climate*, **24**: 4973-4991, doi: 10.1175/2011JCLI4083.1.
- IPCC (Intergovernmental Panel on Climate Change). 2013. Climate Change 2013: The Physical Science Basis. Contribution of Working Group I to the Fifth Assessment Report of the Intergovernmental Panel on Climate Change (Stocker TF, Qin D, Plattner G-K, Tignor M, Allen SK, Boschung J, Nauels A, Xia Y, Bex V, Midgley PM, eds). Cambridge, UK and New York, NY:Cambridge University Press.
- Knutti, R., D. Masson, and A. Gettelman, 2013: Climate model genealogy: Generation CMIP5 and how we got there. *Geophys. Res. Lett.*, **40**, 1194–1199, doi:10.1002/grl.50256.
- Lorenz C., and H. Kunstmann, 2012: The Hydrological Cycle in Three State-of-the-Art Reanalyses: Intercomparison and Performance Analysis. *J. Hydrometeorol*, **13**, 1397–1420.
- Moss, R.H., and co-authors. 2010: The next generation of scenarios for climate change research and assessment. *Nature*, **463**, 747-756 doi:10.1038/nature08823.
- Rasmussen R, and Coauthors. 2011. High-Resolution Coupled Climate Runoff Simulations of Seasonal Snowfall over Colorado: A Process Study of Current and Warmer Climate. *J. Climate*, **24**, 3015–3048.
- Reynolds RW, Smith TM, Liu C, Chelton DB, Casey KS, and Schlax MG. 2007. Daily high-resolution-blended analyses for sea surface temperature. *J. Climate*, **20**: 5473-5496.
- Riahi, K., S. Rao, V. Krey, C. Cho, V. Chirkov, G. Fischer, G. Kindermann, and N. Nakicenovic, 2011: RCP8.5 – A scenario of comparatively high greenhouse gas emissions. *Climatic Change*, **109**, 33–57.
- Skamarock WC, Klemp JB. 2008 A time-split non-hydrostatic atmospheric model for weather research and forecasting applications. *J Comput Phys*, **227**: 3465-3485
- Skamarock WC, Klemp JB, Dudhia J, Gill DO, Barker DM, Duda M, Huang XY, Wang W, Powers JG. 2008. `A description of the Advanced Research WRF Version 3`. NCAR Tech Notes-475+ STR.

Stauffer DR, Seaman NL. 1994. Multiscale four-dimensional data assimilation. *J. Appl. Meteorol.* **33**: 416-434.

Taylor K.E., R.J. Stouffer, and G.A. Meehl, 2012: An Overview of CMIP5 and the Experiment Design. *Bull. Amer. Meteorol. Soc.*, **93**: 485–498 doi:10.1175/BAMS-D-11-00094.1.

Thompson, A. M., K. V. Calvin, S. J. Smith, G. P. Kyle, A. Volke, P. Patel, S. Delgado-Arias, B. Bond-Lamberty, M. A. Wise, L. E. Clarke, and J. A. Edmonds, 2011: RCP4.5: a pathway for stabilization of radiative forcing by 2100. *Climatic Change*, **109**, 77-94.

Xu Z, Yang Z-L. 2012. An improved dynamical downscaling method with GCM bias corrections and its validation with 30 years of climate simulations. *J. Climate* **25**: 6271-6286, doi:10.1175/JCLI-D-12-00005.1.





## 7. Annex: Description of Software for Generating WRF Intermediates

These software scripts and codes were written for this EAD Region Climate Projection project, to enable the development of what are known as 'intermediate' files for the WRF model. These intermediate files are specially formatted so that WRF can make use of them for the regional climate simulations. The codes are summarized below:

### [a. Conversion of CESM to Intermediate Format](#)

This module is called "CCSM4\_TO\_WRFI\_CMIP5\_V3", and is contained in a directory of the same name. Within the directory, the following NCL script reads in CCSM4 data from the CMIP5 archive and writes out the required fields in WRF Intermediate Format:

```
convert_ccsm_hybrid_nc_to_pressure_wrfint_3d.ncl
```

The CESM1 data are stored on glade for easy access. They are for the most part in /glade/p/vetssg/data/CMIP5/output1/NCAR/CCSM4/. You can get an idea of where the exact directories of interest are by looking in the driver script described in the section on how to run the software below. Note that only one CCSM simulation -- Member #6, or 6i1p1 -- has been archived in a manner that the full 6-hourly 3D data required to drive WRF is available. Therefore, you can drive WRF with the data from the 6i1p1 stream, for historical (from 1951-2005) and rcp45, rcp60, and rcp85 (from 2006-2100).

From the NCL script, the following fields are written out at 6-hourly intervals, to Intermediate files called CCSM4\_CMIP5\_MOAR\_CASE:YYYY-MM-DD\_HH, where "CASE" is either 20THC, RCP45, RCP60 or RCP85 and YYYY, MM, DD and HH have their usual time conventions.

### [How to Run CCSM4 TO WRFI CMIP5 V3 Software](#)

[Note: This software has only been tested on NCAR's Yellowstone/Geyser supercomputing platform and instructions below are based on this architecture]

1. *Compile the fortran routine* that is called by NCL via a wrapper:

```
type "./prepare_software.csh" . If successful, the following library file will appear in the "./SRC" directory: write_intermediate.so
```

Note that the fortran code is designed to be compiled using the gnu-based compilers that are packaged with ncl. This shouldn't require any additional modules to be loaded on your part. Specifically, it is required that the intermediate files be written out in big-endian format. Gnu allows a special big-endian flag to be specified in the open statement for the wrf intermediate file within the fortran routine. We did not have any success using other compilers.

2. Make sure you load all of the modules you may need:

```
type "module load ncl"
```

```
type "module load cdo"
```



3. Go to the SEAICE directory and run the `get_seaice.csh` script for your years of interest (submit the script to the geysers queue using `submit_job_to_queue.csh`). Unfortunately, this step is necessary because, as the time these files were created, there was only monthly average sea ice fraction data available on GLADE, and we need at least daily varying sea ice fields in order to have consistent data for our lower boundaries. The only way to get the sea ice is to download it from the HPSS tape storage, which is what this script does.

4. The next step is to simply run the driver script, `run_process_ccsm_to_wrfi.csh`

*4a.: Modify the driver script to specify the years you want to create intermediate files for. The intermediate files are created in 1-year chunks.*

Modify the following line to specify the year or years (separate multiple years by spaces), e.g.:

```
#pick a year
```

```
foreach yyyy (1960 1961)
```

*4b. Run the script.* It takes about 30 min to finish 1 year of data and write out all of the intermediate files. A year of data is 40 Gb. Output files are 6-hourly and named per the convention described above. Note to make sure the following file is in your directory, which allows the SST and SEAICE fields to be interpolated from the POP grid to the CCSM grid: `map_gx1v6_to_fv0.9x1.25_aave_da_090309.nc` (it should be there, so just double check).

```
type "./run_process_ccsm_to_wrfi.csh" .
```

### **b. Conversion of Era-Interim to Intermediate Format**

This module is called "ERA-TO-WRFI-CMIP5-V3". The purpose of this software package is to convert the surface and pressure-level ERA-Interim fields to 1) the same 6-hourly horizontal and vertical domain as the CCSM4 data that was processed in the step above and 2) to Intermediate format. The purpose of this step is to facilitate the bias-correction step, which is described in the following section. The ERA-Interim data used are stored as dataset ds627.0 (6-hourly) and ds627.1 (monthly) on GLADE courtesy of NCAR's Research Data Archive (see the script "run\_process\_era\_to\_wrfi.csh" for details on exact locations of the ERA-Interim data). The procedure to run this software package is nearly identical to that described above for "CCSM4\_TO\_WRFI\_CMIP5\_V3", so details are not provided here to avoid repetition. The ncl script that reformats ERA-Interim ("convert\_era\_grib\_to\_ccsm\_pressure\_wrfint\_3d.ncl") uses the gaussian-to-fixed global grid functions that are available in NCL in order to do the horizontal grid transformation. No vertical interpolation is necessary as all 26 of the vertical pressure levels that are needed to match the CCSM4 vertical levels are already available. All fields are available from the ERA-Interim output at 6-hourly intervals except for "TAVGSFC" which is intentionally derived from the monthly mean ERA-Interim skin temperature in order to maintain stable inland lake surface temperatures.

### **c. Bias-Correction**

This module is written primarily in fortran and performs the Bruyere et al. (2013) bias correction by reading in the CCSM4 and ERA-Interim intermediate files that were created using the two software



packages described above. If researchers from IDEAM or SENHAM are interested in acquiring this dataset, please contact David Yates at [yates@ucar.edu](mailto:yates@ucar.edu).

## Notes on the use of the CESM Intermediate files in WPS and WRF

1. This entire software package is intended to replace the "ungrib.exe" program in WPS, because ungrib.exe cannot handle netcdf input, which is what the CESM data are. Just as ungrib.exe is meant to create WRF intermediate files from grib input, this package creates WRF Intermediate files from netCDF input. You will still be required to run all other steps of WPS and WRF. A typical workflow would be:

Run geogrid.exe after specifying all of your namelist.wps parameters. You should seriously consider modifying the namelist.wps (and possibly GEOGRID.TBL) to allow for the inland lake surface type, which in turn will use the "TAVGSFC" variable to initialize lake surface temperatures. Otherwise, make sure your lake surface temperatures look reasonable. For instructions on how to do this:

see [http://www.mmm.ucar.edu/wrf/users/docs/user\\_guide\\_V3/](http://www.mmm.ucar.edu/wrf/users/docs/user_guide_V3/) >. Note that if you choose to go with the inland lakes option, you *DO NOT* have to run tavg\_sfc.exe per the instructions at this hyperlink -- This has already been done in the NCL script and TAVGSFC is already available to you within the CCSM3D:XXXX-XX-XX\_XX files (therefore, you also *DO NOT* need to add "TAVGSFC" to the 'constants' section of namelist.wps as instructed at the link above).

-- Run the software in this directory *\*instead of ungrib.exe\** to create your intermediate files.

--Run metgrid.exe, making sure that you have properly specified the names of the intermediate files in namelist.wps. You may also want to modify METGRID.TBL to optimize interpolation of SSTs. See Below.

-- Run real.exe from the WRF directory once you have successfully created your met\_em files. Note that you may have to modify "NUM\_LAND\_CAT" in the wrf namelist to reflect the new "lake" land surface type in your dataset. You can find the value of NUM\_LAND\_CAT from doing an ncdump -h of any met\_em file.

-- Run wrf.exe

2. The CCSM data has NO LEAP YEARS. In order to deal with this, if you will be running simulations that span any leap years, you have to add -DNO\_LEAP\_CALENDAR to "ARCH\_LOCAL" in the configure.wps file before compiling WPS (note that some versions of the instructions say to add this flag to "CPPFLAGS" rather than "ARCH\_LOCAL" -- you may have some trial-and-error to figure it out).

3. Downscaling GCM data has a different set of choices regarding simulation strategies than, for example, using WRF for forecasting or hindcasts, since those simulations involve driving WRF with "real" meteorological data rather than GCM data. For starters, some users prefer not to do cold-starts (re-initializations) of WRF every few days as is common for downscaling "real" data. Instead, they might run an entire 20-year period continuously, without any cold starts (in which case they use intermittently-written "RESTART" files to get around wall clock constraints). One advantage of running continuous simulations is that they allow the model soil state to spin up via the land surface model (e.g, the Noah LSM that is coupled to WRF). It typically takes about a year for soil fields to spin up in



the LSM. Another advantage of continuous simulations is that they don't require as much effort for preprocessing, because there are fewer cold-starts to heed; since these are climate model runs, the typical reasons for doing frequent cold starts (e.g., using high fidelity initial conditions to constrain model accuracy with respect to the large-scale driving fields) are not generally first-order considerations. However, you should keep a few things in mind if you choose to do long-term (i.e., greater than a month-long) simulations:

4. Make sure you regularly update fields such as SST using the "sst\_update" flag in your WRF namelist. Otherwise, you might be using January SSTs in July if you initialized a run in January of year X. This software provides 6-hourly TAVGSFC fields so that the inland lakes can be updated along with SSTs (note that although TAVGSFC is written out at 6-hourly intervals for convenience and consistency with other fields, TAVGSFC is actually the *monthly average* skin temperature and therefore only changes on the first day of each month; this approach prevents spuriously large diurnal or day-to-day fluctuations of the lake surface temperatures that can otherwise occur.

5. Think about whether or not spectral or grid nudging (fdda) would be appropriate. This depends on your motives, although one theory is that it may be better not to nudge during long GCM-downscaling runs because the GCMs themselves probably don't have a great representation of the large-scale atmospheric forcing, and thus it may be better to let WRF drift toward its "climatology" inside the model domain. However, it could be advantageous to do fdda nudging if WRF is drifting too much toward unrealistic values over the course of your long simulations. Or, your objective may be to have your simulations be more heavily constrained by the large-scale forcing. In any case, if you do decide to nudge, you should only nudge the upper-most levels (i.e., above ~500 hPa) if you use grid nudging, or use spectral nudging in a manner that you only nudge the large waves. You want to avoid dampening the energy near the surface in WRF -- that is the whole reason for downscaling. Several recent publications suggest that grid nudging, when done properly (only large scale forcing), can improve simulations of extremes in WRF, at least when driving WRF with reanalysis data (see Otte et al., 2012, J. Climate <http://dx.doi.org/10.1175/JCLI-D-12-00048.1>, or Glisan et al., 2013, J. Climate, <http://dx.doi.org/10.1175/JCLI-D-12-00318.1>).

6. You may want to run a "spin-up" year prior to your period-of-interest and then throw it out. This will allow full spin up of the soil state.

7. Fractional sea ice from CCSM has been included in the WRF Intermediate files for your use. As mentioned below, interpolation of sea ice from the comparatively coarse resolution of the CCSM domain to your WRF domain can be tricky. Therefore, be sure to check your sea ice fields in the wrflowbdy\_d0X file once you have interpolated everything onto the WRF domain, to make sure they look realistic, and especially to make sure there aren't issues near coastlines, where masking differences between CCSM and WRF can be problematic. If you choose not to use fractional sea ice, make sure to at least set " seaice\_threshold = 271.35 " (-1.8 C) in the WRF namelist, which will diagnose whether sea ice exists based on whether the SST is less than 271.35.

8. You may have to experiment with some of the interpolation options in METGRID.TBL to refine your subsequent ingest of the WRF intermediate files into metgrid.exe, in order to make sure you get fields in your met\_em files that look right. In particular, masked data -- SST and SEAICE -- interpolation can be tricky near the coastlines when using the comparatively low resolution data from CCSM.



Here are some options (modifications to METGRID.TBL) that seem to work well:

```
=====
name=SST
  interp_option=sixteen_pt+wt_average_16pt+search
  masked=land
  interp_mask = LANDSEA(1)
  fill_missing=-1.E+30
  flag_in_output=FLAG_SST
  missing_value=-1.E+30
=====
```

```
=====
name=SEAICE
  interp_option=four_pt+average_4pt
  interp_mask=LANDSEA(1)
  masked=land
  missing_value=-1.E30
  fill_missing=0.
=====
```

\*\*\*Note that the "search" interpolation option for SST will mean that any \*inland\* lake will take on the SST value from the nearest ocean grid point...this is usually very, very inaccurate. Therefore, if you use this option, make sure to use the inland lakes option ("TAVGSFC") discussed elsewhere in this document.

9. In your namelist.wps file, the following is the correct way to specify the "&metgrid" section (note that everything you should need to run the model is in the CCWM4\_CMIP5\_MOAR\_CASE file, unless you want to use some other fields of your own):

```
&metgrid
fg_name= ' CCSM4_CMIP5_MOAR_CASE' ,
constants_name = ,
io_form_metgrid = 2,
/
```

Or, if you are working with the bias-corrected CCSM output:

```
&metgrid
fg_name= ' CCSM4_CMIP5_MOAR_BC_CASE' ,
constants_name = ,
io_form_metgrid = 2,
```





/

As noted above you may also want to set " geog\_data\_res = 'modis\_lakes+30s', " or " geog\_data\_res = 'usgs\_lakes+30s', " in the &geogrid section of namelist.wps so that you get the inland lakes surface type. This is a must-do action if you plan to use the TAVGSFC field to diagnose inland lake temperatures.

10. Some of the programs in the WPS/util directory may be handy for checking your intermediate files: rd\_intermediate.ext (for seeing what's in them) and plotfmt.exe (for plotting out intermediate data for a quick look)



Climate  
Change  
Research  
Group



NATIONAL CENTER FOR ATMOSPHERIC RESEARCH

LNRClimateChange@ead.ae



an initiative of



هيئة البيئة - أبوظبي  
Environment Agency - ABU DHABI

Abu Dhabi Global Environmental Data Initiative (AGEDI)

P.O Box: 45553

Al Mamoura Building A, Murour Road

Abu Dhabi, United Arab Emirates

Phone: +971 (2) 6934 444

Email : info@AGEDI.ae

agedi.org

